2009

Polarized traffic of LRP1 involves AP1B and SNX17 operating on Y-dependent sorting motifs in different pathways

Maribel Donoso
Pontificia Universidad Catolica de Chile

Jorge Cancino
Pontificia Universidad Catolica de Chile

Jiyeon Lee
Washington University School of Medicine in St. Louis

Peter van Kerkhof
University Medical Center Utrech

Claudio Retamal
Pontificia Universidad Catolica de Chile

See next page for additional authors

Molecular Biology of the Cell
Vol. 20, 481–497, January 1, 2009

Polarized Traffic of LRP1 Involves AP1B and SNX17 Operating on Y-dependent Sorting Motifs in Different Pathways

Maribel Donoso,* Jorge Cancino,* Jiyeon Lee,† Peter van Kerkhof,‡ Claudio Retamal,* Guojun Bu,† Alfonso Gonzalez,*§ Alfredo Cáceres,‖ and María-Paz Marzolo*

*Centro de Regulación Celular y Patología (CRCP), Departamento de Biología Celular y Molecular, Facultad de Ciencias Biológicas, Pontificia Universidad Católica de Chile (PUC) and the Millenium Institute for Fundamental and Applied Biology (MIFAB), Santiago, Chile; †Departments of Pediatrics, and Cell Biology and Physiology, Washington University School of Medicine, St. Louis, MO 63110; ‡Department of Cell Biology and Institute of Biomembranes, University Medical Center, Utrech 3584 CX, The Netherlands; §Departamento de Inmunología Clínica y Reumatología, Facultad de Medicina, Pontificia Universidad Católica de Chile, Santiago, Chile; and ‖Instituto de Investigación Médica Mercedes y Martín Ferreyra (INIMEC-CONICET), Córdoba, Argentina

Submitted August 6, 2008; Revised October 27, 2008; Accepted October 30, 2008
Monitoring Editor: Jean E. Gruenberg

Low-density lipoprotein receptor–related protein 1 (LRP1) is an endocytic recycling receptor with two cytoplasmic tyrosine-based basolateral sorting signals. Here we show that during biosynthetic trafficking LRP1 uses AP1B adaptor complex to move from a post-TGN recycling endosome (RE) to the basolateral membrane. Then it recycles basolaterally from the basolateral sorting endosome (BSE) involving recognition by sorting nexin 17 (SNX17). In the biosynthetic pathway, Y_{29} but not N_{26} from a proximal NPXY directs LRP1 basolateral sorting from the TGN. A $N_{26}A$ mutant revealed that this NPXY motif recognized by SNX17 is required for the receptor's exit from BSE. An endocytic $Y_{63}ATL_{66}$ motif also functions in basolateral recycling, in concert with an additional endocytic motif ($LL_{86,87}$), by preventing LRP1 entry into the transcytotic apical pathway. All this sorting information operates similarly in hippocampal neurons to mediate LRP1 somatodendritic distribution regardless of the absence of AP1B in neurons. LRP1 basolateral distribution results then from spatially and temporally segregation steps mediated by recognition of distinct tyrosine-based motifs. We also demonstrate a novel function of SNX17 in basolateral/somatodendritic recycling from a different compartment than AP1B endosomes.

INTRODUCTION

Epithelial cells posses functional, morphological, and biochemically distinct apical and basolateral cell surface domains and maintain this polarized phenotype addressing specific plasma membrane proteins into each domain (Yeaman *et al.*, 1999; Mostov, 2003; Rodriguez-Boulan *et al.*, 2005). Apical and basolateral proteins are sorted in the biosynthetic route at the level of the *trans*-Golgi network (TGN; Rindler *et al.*, 1984; Fuller *et al.*, 1985; Griffiths and Simons, 1986), and those proteins that undergo endocytosis can be additionally sorted in recycling endosomes (RE; Matter and Mellman, 1994; Mostov and Cardone, 1995; Odorizzi and Trowbridge, 1997). Evidence accumulated over a decade and consolidated in the most recent studies (Ang *et al.*, 2004; Lock and Stow, 2005; Cancino *et al.*, 2007; Cresawn *et al.*, 2007; Gravotta *et al.*, 2007) have shown that the biosynthetic route of at least some proteins includes a post-TGN transit through RE. Under this scenery, it is now important to define the relative contribution of the TGN and RE in the polarized sorting mechanisms of different cargo and in different kind of polarized cells. Neurons, for instance, have to direct distinct proteins to somato-dendritic or axonal plasma membrane domains (Rodriguez-Boulan and Powell, 1992; Winckler and Mellman, 1999), yet their protein-sorting mechanisms remain less known than in epithelial cells. A comparative analysis in epithelial cells and neurons could indeed help to understand the underlying mechanisms of the polarized phenotype.

Studies in MDCK cells, the most currently used model of cell polarity, settled the basics of apical and basolateral protein sorting (Rodriguez-Boulan *et al.*, 2005). Apical membrane proteins possess sorting information located in their extracellular, transmembrane, or cytosolic regions (Rodriguez-Boulan and Gonzalez, 1999; Marzolo *et al.*, 2003), and their polarized sorting has been mainly linked to lipid raft association (Fullekrug and Simons, 2004) and glycosylation (Fiedler and Simons, 1995). Glycosylation-independent apical pathways have been also reported (Marzolo *et al.*, 1997, 2003; Rodriguez-Boulan and Gonzalez, 1999; Bravo-Zehnder *et al.*, 2000; Marmorstein *et al.*, 2000). In contrast, basolateral transmembrane proteins hold discrete sorting signals exclu-

This article was published online ahead of print in *MBC in Press* (http://www.molbiolcell.org/cgi/doi/10.1091/mbc.E08–08–0805) on November 19, 2008.

Address correspondence to: María-Paz Marzolo (mmarzolo@bio.puc.cl).

sively in their cytoplasmic domains and frequently based on tyrosine (NPxY, Yxxϕ) or dihydrophobic (LL; IL) residues. Noncanonic basolateral motifs lacking any consensus sequence have been also described (Casanova *et al.*, 1991; Aroeti and Mostov, 1994; Le Gall *et al.*, 1997; Odorizzi and Trowbridge, 1997; Deora *et al.*, 2004). In addition, many basolateral proteins possess recessive apical-sorting information that becomes apparent after abrogation of their basolateral motifs (Rodriguez-Boulan *et al.*, 2005). The frequent finding that Y-dependent basolateral motifs are collinear with endocytic determinants has for a long time suggested that the basolateral and the endocytic-sorting machineries share some common elements (Hunziker and Fumey, 1994; Matter and Mellman, 1994; Matter *et al.*, 1994; Rodriguez-Boulan *et al.*, 2005). Studies involving clathrin adaptors (Folsch *et al.*, 1999; Ohno *et al.*, 1999; Simmen *et al.*, 2002) and, most recently clathrin itself, (Deborde *et al.*, 2008) in basolateral sorting support this notion.

Because the TGN and endosomal compartments cooperate in the process of polarized protein sorting (Rodriguez-Boulan *et al.*, 2005), it is important to define where and how the variety of sorting signals become decoded. In MDCK cells, newly synthesized apical and basolateral membrane proteins segregate first at the TGN (Rodriguez-Boulan *et al.*, 2005). Then, membrane proteins leaving the Golgi apparatus may traverse RE compartments before arrival to the cell surface. This pathway has been better documented for basolateral proteins (Ang *et al.*, 2004; Lock and Stow, 2005; Cancino *et al.*, 2007; Gravotta *et al.*, 2007). At least for some basolateral proteins, such as the transferrin receptor (TfR) and vesicular stomatitis virus glycoprotein (VSVG) protein, but not the low-density lipoprotein receptor (LDLR), biosynthetic trafficking through RE seems to be an obligate station (Cancino *et al.*, 2007). Some apical proteins may also pass through endosomal intermediates (Cresawn *et al.*, 2007). Once at the plasma membrane, proteins internalized from each cell surface domain can be recycled back to the same domain or transported by transcytosis to the opposite pole (Matter *et al.*, 1993; Aroeti and Mostov, 1994; Matter and Mellman, 1994; Mostov and Cardone, 1995; Odorizzi and Trowbridge, 1997). Again, this view mainly derives from observations in basolateral proteins, as many of them are also endocytic proteins that recycle several times without losing polarity (Rodriguez-Boulan *et al.*, 2005), indicating that they are sorted first during their biosynthetic trafficking and then several times during recycling (Matter *et al.*, 1993; Gan *et al.*, 2002; Marzolo *et al.*, 2003; Cancino *et al.*, 2007; Gravotta *et al.*, 2007).

Studies on the LDLR (Matter *et al.*, 1993) and polymeric immunoglobulin receptor (pIgR; Aroeti and Mostov, 1994) led to the concept that the same sorting motifs are used both at the TGN and recycling endosomes. However, the TfR seems to use distinct motifs at these locations (Odorizzi and Trowbridge, 1997). The sorting machinery of the TGN can discriminate between different basolateral sorting signals in vitro (Müsch *et al.*, 1996) and in vivo (Soza *et al.*, 2004) and could in principle also discriminate between otherwise similar basolateral and recycling motifs. So far, the proteins involved in decoding basolateral sorting signals have been the widely expressed AP4 complex (Simmen *et al.*, 2002) and the clathrin adaptor complexes AP1B complex specifically expressed by certain epithelial cells (Folsch *et al.*, 1999; Ohno *et al.*, 1999; Gan *et al.*, 2002), both acting predominantly upon Y-dependent motifs. AP1B has been localized in TfR-containing recycling endosomes as part of the sorting machinery operating in post-TGN biosynthetic and recycling pathways (Cancino *et al.*, 2007; Gravotta *et al.*, 2007). It is necessary to extend the analysis of the sorting signals that could operate at the TGN and/or endosomes and to search for additional decoding elements that might be involved in distinct endocytic compartments.

All these aspects are less known in neurons, even though they are considered to share elements of the sorting machinery with epithelial cells (Horton and Ehlers, 2003; Silverman *et al.*, 2005). There are several examples of apical and basolateral proteins handled, respectively, as axonal and somatodendritic proteins in neurons, and vice versa in epithelial cells (Dotti and Simons, 1990; Dotti *et al.*, 1991; Pietrini *et al.*, 1994; Bradke and Dotti, 1998). However, there are also examples that do not fit into this pattern. For example, there is evidence suggesting that neurons cannot interpret dihydrophobic sorting signals as epithelial cells do (Silverman *et al.*, 2005). Interestingly, even though neurons do not express AP1B (Ohno *et al.*, 1999), they still direct proteins to dendrites, such as the TfR (Bradke and Dotti, 1998), LDLR (Jareb and Banker, 1998), and LDLR-related protein 1 (LRP1; Brown *et al.*, 1997), whose basolateral distribution in epithelial cells is AP1B-dependent (Folsch *et al.*, 1999; Gan *et al.*, 2002; Marzolo *et al.*, 2003).

The variety of functions played by LRP1 and what we known about its trafficking behavior makes it an interesting model protein to explore how epithelial cells and neurons organize their protein-sorting machineries. This receptor is essential for early embryonic development (Herz *et al.*, 1992, 1993) and also plays roles in blood coagulation, cell adhesion and migration, neuronal process outgrowth, and the pathogenesis of Alzheimer's disease (Hussain, 2001; Herz and Bock, 2002). LRP1 ligands include proteinases, proteinase-inhibitor complexes, lipoprotein particles, amyloid precursor protein, and extracellular matrix proteins (Bu *et al.*, 1992; Godyna *et al.*, 1995; Hussain, 2001; Salicioni *et al.*, 2002; Brandan *et al.*, 2006). On binding, LRP1 mediates catabolism of these ligands and/or their signal transduction effects (Goretzki and Mueller, 1998; Bacskai *et al.*, 2000; Zhuo *et al.*, 2000). LRP1 is expressed broadly, being basolateral in epithelial cells and somato-dendritic in neurons (Brown *et al.*, 1997; Marzolo *et al.*, 2003).

We previously described that basolateral sorting of LRP1 depends on two critical tyrosine residues (Y_{29} and $Y_{63,}$ after the first amino acid residue of the cytoplasmic domain after the transmembrane domain) and the adaptor complex AP1B (Marzolo *et al.*, 2003). Studies in nonpolarized cells have shown that $Y_{63,}$ within the YATL motif, contributes to the very fast internalization of LRP1 (Li *et al.*, 2000). It is important to define whether Y_{63} operates as a basolateral signal within the context of $NPxY_{63}$ or $Y_{63}xx\phi$ motifs that share this residue (Marzolo *et al.*, 2003). In addition, our studies in nonpolarized cells demonstrated that Y_{29} belongs to a recycling motif $N_{26}PxY_{29}$ that provides a binding site for sorting nexin 17 (SNX17). These studies also showed that SNX17 is required for LRP1 recycling (van Kerkhof *et al.*, 2005 3518). SNX17 belongs to a family of proteins involved in sorting processes (Worby and Dixon, 2002) and binds to the cytosolic domain of several LDLR family members (Stockinger *et al.*, 2002). However, the role of SNX17 and its binding motif $N_{26}PxY_{29}$ has not been explored in polarized cells, neither in epithelial cells nor in neurons. Actually, no sorting signal has been identified as somatodendritic determinant in LRP1 (Brown *et al.*, 1997). Thus, LRP1 provides unique opportunities to study the relative contribution of different motifs in basolateral sorting processes taking place at the TGN and at post-TGN pathways, including AP1B- and SNX17-containing endocytic compartments. It is also an interesting model

protein to assess the role of SNX17 in the sorting machinery of epithelial cells and neurons.

MATERIALS AND METHODS

Materials

All tissue culture media, serum, and plastic ware were from Invitrogen (Carlsbad, CA). Tissue culture-treated Transwell polycarbonate filters were from Costar (Costar, Cambridge, MA). Complete protease inhibitor tablets were from Roche Applied Science (Indianapolis, IN). Rabbit polyclonal anti-human LRP1 (RRR) and the monoclonal anti-HA antibody have been described before (Obermoeller *et al.*, 1998). Monoclonal anti-HA (12CA5) was from BabCO (Richmond, CA). Polyclonal anti-HA antibody was from Upstate Biotechnology (Lake Placid, NY) and a rabbit polyclonal anti-HA (HA, Y-11) was from Santa Cruz Biotechnology (Santa Cruz, CA). Monoclonal anti-myc (9E10) was purchased from Roche Diagnostics (Alameda, CA). Mouse anti-E-cadherin mAb was from BD Biosciences (San Jose, CA). Rat anti-uvomorulin/E-cadherin and mouse anti-acetylated tubulin (clone 6-11B-1) monoclonal antibodies were from Sigma Chemical (St. Louis, MO). Polyclonal anti-human megalin was generated against a recombinant megalin tail obtained as described previously (Marzolo *et al.*, 2003). Human serum with reactivity against EEA1 was obtained from a patient with systemic lupus erythematosus controlled in our rheumatology laboratory. Rabbit anti-human SNX17 was made against the peptide "HGNFAFEGIGDEDL" present in the carboxyl terminal region. This sequence is completely conserved between human and mouse SNX17 and does not have homology to other proteins. μ1B-specific blocking-function antibody was previously described (Cancino *et al.*, 2007) and recognized the human as well as the rat adaptor subunit. The secondary antibodies sheep anti-mouse– and goat anti-rabbit–conjugated to horseradish peroxidase (HRP) were from Chemicon (Temecula, CA). The mAb against MAP2 (clone AP14, mouse IgG) was described previously (Caceres *et al.*, 1992). Cy-3–conjugated goat anti-mouse IgG was from Chemicon. Alexa488- and Alexa594-conjugated goat anti-rabbit antibodies, goat anti-chicken Alexa594, and goat anti-mouseAlexa350 were obtained from Molecular Probes (Leiden, The Netherlands). TRITC-conjugated goat-anti-human IgG was from Sigma Chemical. EZ-link Sulfo-NHS-LC-biotin, EZ-link Sulfo-NHS-SS-biotin, and Immunopure streptavidin-agarose were from Pierce Biochemical (Rockford, IL). Protein A-agarose was from Repligen (Waltham, MA). Immobilon-P transfer membrane was from Millipore (Billerica, MA). Kaleidoscope molecular weight markers were from Bio-Rad (Hercules, CA). The ECL system was from Amersham Pharmacia Biotech (Piscataway, NJ).

Construction of LRP1 Minireceptors

All the constructs have the hemagglutinin (HA) epitope in their amino termini and are composed of the fourth ligand binding, transmembrane and cytoplasmic domains of LRP1 (mLRP4). The construction of wild-type and mutant forms of the minireceptor ($N_{26}A$, $Y_{29}A$, $LL_{43,44}AA$, $N_{60}A$, $Y_{63}A$, $L_{66}A$, $S_{76}A$, $LL_{86,87}AA$, and $Y_{63}A/LL_{86,87}AA$), have already been described (Li *et al.*, 2000, 2001a,b). The new mutant mLRP4 $DD_{38,39AA}$ was made using the QuickChange site-directed mutagenesis kit from Stratagene, according to the manufacturer's instructions. The oligonucleotides synthesized at the Washington University School of Medicine Protein Chemistry Laboratory. All the constructs were verified by DNA sequencing.

Plasmids for the Expression of μ1B-HA and myc-SNX17 and of a Dominant Negative Form of eps15

The plasmid encoding μ1B with an internal HA tag was kindly provided by Dr. Ira Mellman (Folsch *et al.*, 2001). The plasmid encoding the myc-tagged SNX17 was obtained as described (van Kerkhof *et al.*, 2005). The expression plasmid for GFP-EPS15 DD (EΔ95/295), a dominant form of eps15 (D/N-eps15; Benmerah *et al.*, 1999) was kindly provided by Dr. Alexander Benmerah (Institut Cochin-U567 INSERM/UMR8104 CNRS-Paris, France).

Cell Culture Conditions and Transfection

Madin-Darby canine kidney (MDCK) cells (strain II) were maintained in DMEM (Invitrogen) supplemented with 7.5% fetal bovine serum (FBS; Invitrogen) containing 100 U/ml penicillin and 100 mg/ml streptomycin sulfate. Fisher rat thyroid (FRT) cells were grown in Coon's modified F12 medium with 10% FBS and antibiotics as described (Marzolo *et al.*, 1997). Clonal cell lines were derived from MDCK and FRT cells stably transfected with 2 μg DNA by using Lipofectamine Plus transfection reagent (Invitrogen) according to the supplier's protocol, followed by 10–14 d of selection with 0.8 mg/ml G418 (Invitrogen). Cells were screened and analyzed by Western blot and indirect immunofluorescence as described below. Selected clones were maintained in the same medium plus 0.4 mg/ml G418.

Hippocampal neurons were cultured as described (Banker and Cowan, 1977). Dissociated cells were plated on glass coverslips coated with 1 mg/ml poly-L-lysine in medium containing 10% horse serum (Invitrogen-BRL). After 3 h, the medium was supplemented with N2 (Invitrogen-BRL; Bottenstein and Sato, 1979). Cells were transiently transfected at 7 d using LipofectAMINE 2000 (Invitrogen) (Paglini *et al.*, 1998). Cells were then analyzed at different posttransfection intervals ranging from 12 to 18 h.

For most of the experiments related to epithelial polarity analysis, cells were plated at high density onto 12- or 24-mm Transwell polycarbonate filter units (0.4-μm pore size). Cells were grown until the transepithelial resistance reached 200–350 Ù/cm² for MDCK cells, 5000–8000 Ù/cm² for FRT cells, measured with an EVOM electrometer (World Precision Instruments, Sarasota, FL). The formation of a properly polarized monolayer of MDCK cells was determined by the analysis of the lateral expression of E-cadherin either by indirect immunofluorescence or by biotinylation, as indicated.

Immunofluorescence Microscopy

MDCK and FRT cells were plated at 1×10^5 on glass coverslips in 24-well dishes and grown for 3 d. Cells were fixed in 2% paraformaldehyde (PFA) in PBSc (phosphate-buffered saline containing 0.1 mM calcium and 1 mM magnesium) and then permeabilized or not with 0.2% Triton X-100 in PBSc. Before being incubated with the primary antibody, cells were blocked with 0.2% gelatin in PBS. Successive incubations with the first antibody and Cy3 or Alexa 488 secondary antibody were carried out. After washing with PBS and with 0.2% gelatin in PBS, the coverslips were mounted with Mowiol (Calbiochem, San Diego, CA).

Hippocampal neurons were fixed with 4% PFA and 4% sucrose for 20 min at 37°C, and processed for immunofluorescence as described previously (Rosso *et al.*, 2004). For cell surface staining, incubation with primary or secondary antibodies was performed before permeabilization with detergents. Stained cells were observed and analyzed with an inverted microscope (Carl Zeiss, Thornwood, NY; Axiovert 35M) equipped with epifluorescence and photographed using a 63× objective (Carl Zeiss) using Axiovision (version 3.0.6), or a Zeiss laser scanning confocal microscope. X-Y sections, in 0.45-μm steps, were collected sequentially at 1024×1024 resolution.

Cell Surface Biotinylation and Flow Cytometry in Epithelial Cell Lines

The cell surface distribution of the receptors was assessed by cell surface biotinylation, immunofluorescence, and flow cytometry. Cell surface biotinylation was performed at 4°C, as described (Le Bivic *et al.*, 1989; Marzolo *et al.*, 2003). Briefly, the cell monolayers grown on filters were washed in PBSc and then biotinylated with sulfo-NHS-LC-biotin from either the apical (0.7 ml) or basolateral (1.5 ml) chamber compartment. The chamber not receiving biotin was incubated with PBSc. Filters were incubated twice for 30 min. After biotinylation steps, biotin was quenched by incubation with 50 mM NH_4Cl in PBSc for 10 min. Cells were lysed in ice-cold lysis buffer (150 mM NaCl, 20 mM Tris, pH 8.0, 5 mM EDTA, 1% Triton X-100, 0.2% BSA, and protease inhibitors). Biotinylated cell surface proteins were then adsorbed to streptavidin-agarose beads for 2 h. Beads were washed, and the biotinylated proteins analyzed by SDS-PAGE followed by immunoblotting (see below). For analysis of the cell surface receptor by flow cytometry, MDCK cells expressing the different minireceptors were grown on 100-mm dishes until 80% confluent. The cells were detached by incubation with PBS/5 mM EDTA and trypsin. Detection of cell surface minireceptor was performed by using monoclonal anti-HA antibody, followed by incubation with goat anti-mouse R-phycoerythrin (RPE) antibody (Dako, Glostrup, Denmark). The total amount of receptor expressed en each cell was assessed in cells previously permeabilized with PBS 0.1% saponin. Background fluorescence intensity was assessed in the absence of primary antibody and subtracted. Mean fluorescence values were obtained in triplicate with a FACScalibur (BD Biosciences-PharMingen, Sweden), and data were analyzed with Cell Quest software (BD Biosciences-PharMingen).

Immunoblotting and Coimmunoprecipitation Assays

For Western blotting, cells were lysed with lysis buffer (PBS containing 1% Triton X-100, 1 mM PMSF, 1 μg/ml each of pepstatin, antipain, leupeptin, and aprotinin) for 1 h at 4°C. Lysates were resolved by SDS-PAGE under reducing conditions, transferred to polyvinylidene difluoride (PVDF) membrane, and incubated with the corresponding primary antibody (mouse anti-HA 1:200 for the 12CA5 mAb and 1:500 for the BabCO antibody, anti-human LRP1 1:500, anti-E-cadherin 1:1000, mouse anti-myc 1: 500) overnight at 4°C. Membranes were washed, incubated with species-specific secondary antibodies conjugated to HRP (anti-mouse HRP 1:5000 and anti-rabbit HRP 1:10000) for 1 h at room temperature, and immunoreactive proteins were detected using the ECL system.

For the coimmunoprecipitation, cells were grown to subconfluence on 10-cm tissue culture dishes. Cells were rinsed twice with cold PBS and lysed in 800 μl of buffer lysis (150 mM NaCl, 50 mM HEPES, pH 7.5, 10% glycerol, 1 mM EGTA, 1% Triton X-100, 1.5 mM $MgCl_2$, 100 mM NaF, 10 mM sodium pyrophosphate, 500 μM orthovanadate, 1 mM PMSF, 1 mM aprotinin, 1 mM leupeptin, and 1 mM pepstatin). Lysates were cleared by centrifugation at 10,000 rpm at 4°C, incubated with 10 μg of anti-LRP1 or anti-MegT antibody (Marzolo *et al.*, 2003) for 2 h at 4°C, and subsequently mixed with 40 μl of protein A-Sepharose for 1 h at 4°C. Sepharose beads were collected by

centrifugation and washed three times with lysis buffer. Immunoprecipitates were boiled 3 min and resolved by SDS-PAGE and immunoblotting.

Cell Surface Fluorescence Quenching Recycling Assay

This assay was basically performed as described (van Kerkhof *et al.*, 2005). In our assay we also included nontransfected cells to subtract the nonspecific fluorescence. MDCK cells, wild-type and stably expressing minireceptors were incubated with Alexa488-labeled anti-HA antibodies for 20 min at 37°C. After removal of fluorescent antibody in the medium, the cells were incubated for the indicated time periods (0–10 min) in the absence or presence of 24 μg/ml anti-Alexa488 IgG (Molecular Probes) to quench the fluorescence and then rapidly chilled, detached, and analyzed by flow cytometry for fluorescence intensity. Background fluorescence intensity assessed in the absence of primary antibody was subtracted. Mean fluorescence values were obtained in triplicate with a FACScalibur (BD Biosciences-PharMingen), and data were analyzed with Cell Quest software (BD Biosciences-PharMingen). The percentage of initial fluorescence (pulse) remaining at each time point was calculated as the difference between nonchased (time 0) and chased cell fluorescence and then normalized to the nonchased value in order to calculate the % of recycling efficiency.

Microinjection Experiments

Minireceptor's Trafficking Assays. The microinjection approach to express and accumulate exogenous cargo at the TGN and then to assess its subsequent trafficking to the plasma membrane, was performed essentially as described (Kreitzer *et al.*, 2000; Cancino *et al.*, 2007). MDCK and FRT cells were plated at subconfluent levels on glass coverslips and microinjected after 3 d of reaching confluence. The expression plasmids (25 μg/ml) and antibodies (40 μg/ml) were dissolved in HKCl microinjection buffer (10 mM HEPES, 140 mM potassium chloride, pH 7.4). Microinjections were performed in the cell nucleus (plasmids) and cytosol (antibodies) using back-loaded glass capillaries and an Eppendorf Transjector 5246 system mounted on a Zeiss Axiovert S100 inverted microscope, keeping the cells in bicarbonate-free DMEM supplemented with 5% FBS, 20 mM HEPES, pH 7.4. The microinjected cells were incubated for 1 h at 37°C, and newly synthesized protein was accumulated in the TGN at 20°C for 2 h in the presence of 100 μg/ml of cycloheximide. After the 20°C block the cells were incubated for different times at 37°C to resume TGN-to-cell-surface protein traffic and then fixed with 4% PFA in PBS-CM buffer for 30 min. The cells were then incubated with rabbit polyclonal anti-HA antibody before permeabilization for 30 min. Cells were washed twice 5 min with PBS and refixed in 4% PFA for 15 min and then permeabilized with 0.2% Triton X-100 for 10 min. The cells were then incubated with chicken anti HA-antibody for 30 min. The apical localization of mini-receptors was detected with secondary goat anti-rabbit-Alexa488 or goat anti-rabbit-Alexa555 antibodies. Intracellular/basolateral localization of mini-receptors was detected with goat anti-chickenAlexa-594 antibody. Confocal microscopy was performed using a laser scanning LSM 510 Zeiss microscope, 63× oil immersion lens, at 22°C. Images were processed using MetaMorph software version 6.0r1.

B) Colocalization Analysis. MDCK cells were microinjected as above with plasmids for the expression of RAP, SNX17-myc and HA-tagged minireceptors. The microinjected cells were incubated for 2 h at 37°C, newly synthesized proteins were left 2 h in the presence of 100 μg/ml of cycloheximide, and then cells were fixed, permeabilized and stained with rabbit anti-HA, mouse anti-myc and human anti-EEA1 antibodies. The secondary antibodies used were goat-anti-mouse-Alexa350, goat-anti-rabbit-Alexa488 and goat-anti-human TRITC. Images were captured in a Zeiss Axiophot microscope using 100x lens and Axiocam camera. Images were processed using MetaMorph software version 6.0r1. For quantification, all images from a single experiment, five for each coverslip, were acquired under identical settings (14 bits; 1300 × 1030 pixels, and the same exposure times, avoiding signal saturation), and their integrated fluorescence intensities (equivalent to the sum of all grayscale values for every pixel in the region) ere analyzed after 2D deconvolution and threshold adjustment to select positive staining for each fluorescent probe. The percentage of colocalization, measured as integrated pixel intensity in the regions of overlap, of mLRP4 and mLRP4N26A with EEA-1 and SNX17 was calculated for each individual cell (n = 30). Objects with saturated pixels were omitted from quantifications.

Transcytosis Assay

To assess basolateral-to-apical transcytosis, we applied a described strategy that uses sulfo-NHS-SS-biotin and glutathione stripping (Burgos *et al.*, 2004) with modifications. Cells were grown in transwell filters until confluent. On the day of the experiment, cells were washed two times with ice-cold PBSc for 5 min, and the basolateral domain was biotinylated with 1 mM of the cleavable sulfo-NHS-SS-biotin for 20 min at 4°C. The reaction was then quenched twice with 50 mM NH_4Cl for 10 min at 4°C. After three washes with PBSc for 5 min each, the cells were incubated with DMEM/HEPES for 45 min at 37°C and then chilled and washed again three times with ice-cold PBS. The biotin of proteins appearing at the apical cell surface was stripped with 50 mM GSH, added twice to the apical compartment for 30 min at 4°C. Reduction was also performed at the basolateral domain in different filters as control. The reaction was stopped by washing with PBS and incubating with 5 mg/ml iodoacetamide in PBS, containing 10% BSA, for 30 min at 4°C. Cells were washed with PBS three times and then were lysed in ice-cold lysis buffer containing 2.5 mM iodoacetamide for 1 h at 4°C. Lysates were centrifuged at 14,000 rpm for 10 min at 4°C and incubated with streptoavidin beads as in the biotinylation protocol. Precipitated proteins were identified by Western blot with anti-HA to detect the minireceptors and anti-E-cadherin to control loading and domain specific reduction. All the experiments were repeated three times, with 1–2 filters per point, depending on the expression level of the minireceptor analyzed. The band corresponding to the minireceptor in each condition was quantified by densitometry. The transcytosis efficiency was determined after 45 min of basolateral-to-apical trafficking at 37°C after the basolateral biotinylation, as follows: Basolateral-to-apical transcytosed minireceptor = Total basolaterally biotinylated minireceptor − Biotinylated minireceptor remaining after reduction at the apical surface. Basolaterally Recycled receptor = Total Basolaterally Biotinylated receptor − Biotinylated minireceptor remaining after reduction at the basolateral surface.

RESULTS

LRP1 Is Transported to the Basolateral Surface in MDCK and FRT Cells

To assess the sorting behavior of LRP1, we used HA-tagged minireceptors containing the fourth ligand binding domain, the transmembrane domain, and the cytoplasmic tail of the receptor (mLRP4; Marzolo *et al.*, 2003). We first examined whether two different epithelial cell lines, MDCK and FRT, of kidney and thyroid origin, respectively, express and sort endogenous LRP1 similarly. The LRP1 antibody against the human protein readily localized the endogenous LRP1 in the basolateral domain of MDCK cells, as we previously described (Marzolo *et al.*, 2003; Figure 1A). In contrast, FRT cells showed much lower expression levels (not shown). However, both cell lines distributed the transfected mLRP4 predominantly in the basolateral domain (Figure 1B), indicating similar decoding of the LRP1 basolateral sorting information.

AP1B Regulates LRP1 Trafficking at a Post-Golgi Recycling Endosome

We have previously shown that LLC-PK1 cells, which lack the adaptor subunit μ1B of the AP1B complex that recognizes tyrosine-based basolateral sorting motifs (Ohno *et al.*, 1999), distributes LRP1 in a nonpolarized manner unless exogenous μ1B is expressed by transfection (Marzolo *et al.*, 2003). To determine whether LRP1 interacts with AP1B, we transiently transfected MDCK cells with HA-μ1B and then LRP1 was immunoprecipitated from the cell lysates. The adaptor complex subunits, HA-μ1B and γ-adaptin, were found in the immunoprecipitates (Figure 2A), suggesting that LRP1 does interact with AP1B.

We recently reported that an anti-μ1B antibody is able to block the biosynthetic trafficking of VSVG and TfR at a μ1B-containing RE that most likely represents the common recycling endosome (CRE) in FRT cells, 5–10 min after exiting the TGN (Cancino *et al.*, 2007). The antibody also blocked the postendocytic trafficking of LDLR at μ1B-RE. Here we performed similar experiments to define which μ1B-dependent route is used by LRP1. FRT cells were microinjected with mLRP4 and RAP plasmids with or without anti μ1B antibody. After 1 h of synthesis at 37°C, 2 h of TGN accumulation at 20°C, and 1 h of releasing the TGN block at 37°C, the mLRP4 achieved a basolateral distribution that contrasted with the perinuclear retention caused by the μ1B antibody (Figure 2B). This experiment revealed a μ1B-dependence of LRP1 trafficking at μ1B-RE but did not allow to define whether this occurs immediately after exiting the TGN or after endocytosis. A time course experiment re-

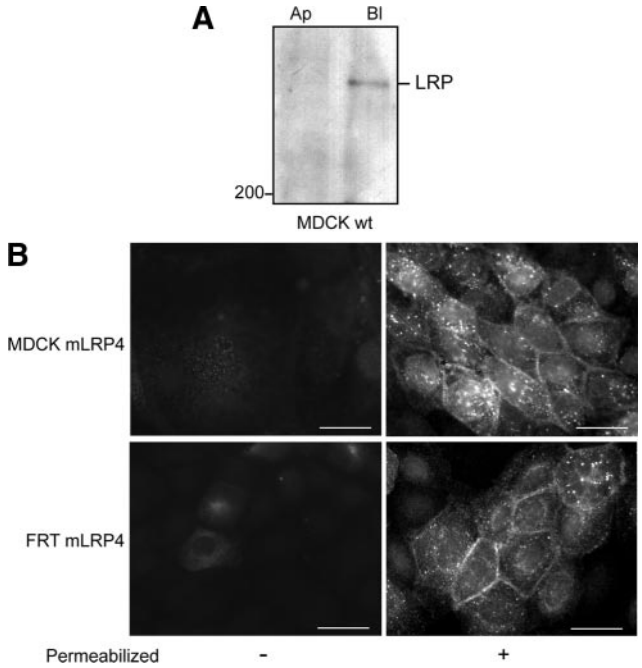

Figure 1. Basolateral expression of LRP1 and its minireceptors in polarized epithelial cells. (A) MDCK cells biotinylated either at the apical (Ap) or basolateral (Bl) domain at 4°C were lysed, and the surface biotinylated proteins were precipitated with streptavidin-agarose and resolved in 5% SDS-PAGE followed by immunoblot with anti-human LRP1. Endogenous LRP1 distributes at the basolateral domain. (B) MDCK and FRT cells stably expressing the mLRP4 minireceptor were grown until confluent on coverslips, and the distribution of the minireceptor was visualized by indirect immunofluorescence with monoclonal anti-HA. The minireceptor was detected only after cell permeabilization at the basolateral cell borders and in intracellular vesicles. Scale bars, 10 μm.

solved this question (Figure 2, C and D). Before releasing from the 20°C TGN block, the receptor does not colocalize with μ1B. After 5 min of TGN block release, more than 50% of mLRP4 colocalizes with μ1B in a perinuclear compartment and reaches up to a 75% of colocalization at 10 min, maintaining this distribution even after 1 h at 37°C. These results indicate that after exiting the TGN the LRP1 is first transported to the μ1B-RE while en route to the basolateral cell surface, thus sharing with VSVG and TfR this indirect basolateral pathway (Cancino *et al.*, 2007).

Identification of Sorting Motifs in the LRP Cytoplasmic Domain

To define sorting motifs within the LRP1 cytoplasmic domain, as well as the context sequence of the basolateral information conveyed by the Y_{29} and Y_{63} residues (Marzolo *et al.*, 2003), we analyzed new site-directed mutants of LRP1 minireceptors, as depicted in Figure 3, The wild-type minireceptor mLRP4 has a cytoplasmic domain composed of 100 amino acids containing several putative sorting motifs (Figure 3). These include two NPxY motifs ($N_{26}PTY_{29}$ and $N_{60}PVY_{63}$), one YxxΦ ($Y_{63}ATL_{66}$) motif that shares the tyrosine with the $N_{60}PVY_{63}$ motif, two dileucine motifs ($LL_{43,44}$ and $LL_{86,87}$), and a pair of negatively charged amino acids ($DD_{38,39}$), similar to those involved in LDLR basolateral sorting (Matter *et al.*, 1992). There is also a protein kinase A (PKA) phosphorylation site involving the serine in position 76 (S_{76}) that has a role in LRP endocytosis (Li *et al.*, 2001b).

We generated stable MDCK cells lines and assessed the steady-state distribution and trafficking properties of the different minireceptor constructs by analyzing two or three MDCK clones for each construct. The results of domain specific biotinylation assays are presented from the proximal to distal location of the analyzed motifs (Figure 4). As described (Marzolo *et al.*, 2003), the mutation in the first NPxY motif ($NPTY_{29}A$) completely redistributes LRP1 to the apical domain. Neither the $DD_{38,39AA}$ mutant nor the $LL_{43,44}AA$ mutant affected the LRP1 basolateral distribution. However, a truncated LRP1 construct lacking the last 41 amino acids revealed a potential basolateral sorting function of $DD_{38,39}$ residues (data not shown). The already described mutation of the Y_{63} residue leads to a nonpolarized distribution of the receptor (Marzolo *et al.*, 2003). This tyrosine is shared by the distal $N_{60}PVY_{63}$ motif and the endocytic motif $Y_{63}ATL_{66}$ (Li *et al.*, 2000). Here, we determined that its basolateral sorting function is exerted independently of N_{60}, since the $N_{60}A$ mutant distributed predominantly basolateral. Instead, the $L_{66}A$ mutation mistargeted the receptor to the apical domain by more than 50%. Thus, Y_{63} constitutes a YxxΦ and not a NPxY basolateral sorting motif.

In nonpolarized cells, the $Y_{63}ATL_{66}$ and $LL_{86,87}$ motifs contribute independently to the rate of LRP1 endocytosis (Li *et al.*, 2000). We found here that $LL_{86,87}$ is also required for LRP1 basolateral distribution. The mutant $LL_{86,87AA}$, similarly to the $Y_{63}A$ mutant, showed a nonpolarized distribution. Furthermore, the double mutant $Y_{63}A/LL_{86,87AA}$ also distributed in a nonpolarized manner. Neither of these motifs seem to compensate for the loss of function of the other. These signals seem to act in concert, as if forming part of a single complex sorting signal. Finally, the unique PKA phosphorylation site S_{76} was not required for LRP1 basolateral sorting.

These results define the context of the previously described Y_{63}-dependent basolateral sorting signal and revealed novel sorting requirements involving L_{66} and $LL_{86,87}$ residues. The contrasting apical segregation of $Y_{29}A$ and nonpolarized distribution of $Y_{63}A$ and $LL_{86,87}AA$ mutants prompts to further analyzing the proximal NPxY motif and the sorting pathways where these motifs exert their function.

The Basolateral Information Conveyed by Y_{29} Operates at the TGN

The different phenotypes produced by alanine replacement in either the Y_{29} or the Y_{63} and $LL_{86,87}$ residues suggest that sorting signals associate with temporally–spatially compartmentalized functions. An interesting possibility is that the Y_{29}-dependent motif operates during biosynthetic trafficking at the TGN level, whereas Y_{63} and $LL_{86,87}$ operates biosynthetically in a post-TGN station and/or at a basolateral recycling route after internalization. In this hypothetic model, mutant receptors lacking the function of Y_{63} or $LL_{86,87}$ residues would be targeted basolaterally from TGN due to the Y_{29}-dependent sorting, but would enter into basolateral-to-apical transcytotic pathways and lose polarity during postendocytic recycling.

To test the hypothesis that the Y_{29}-dependent motif acts at the biosynthetic route, we performed cDNA microinjection experiments in MDCK cells grown on glass coverslips and microinjected after 3 d of reaching confluence. Under these conditions the cells are properly polarized, as is shown by the basolateral distribution of E-cadherin and the presence of detectable primary cilium, which is labeled with a mAb recognizing acetylated tubulin (Supplemental Figure S1). We used an established approach that assesses transport from the TGN to the cell surface (Kreitzer *et al.*, 2000). The

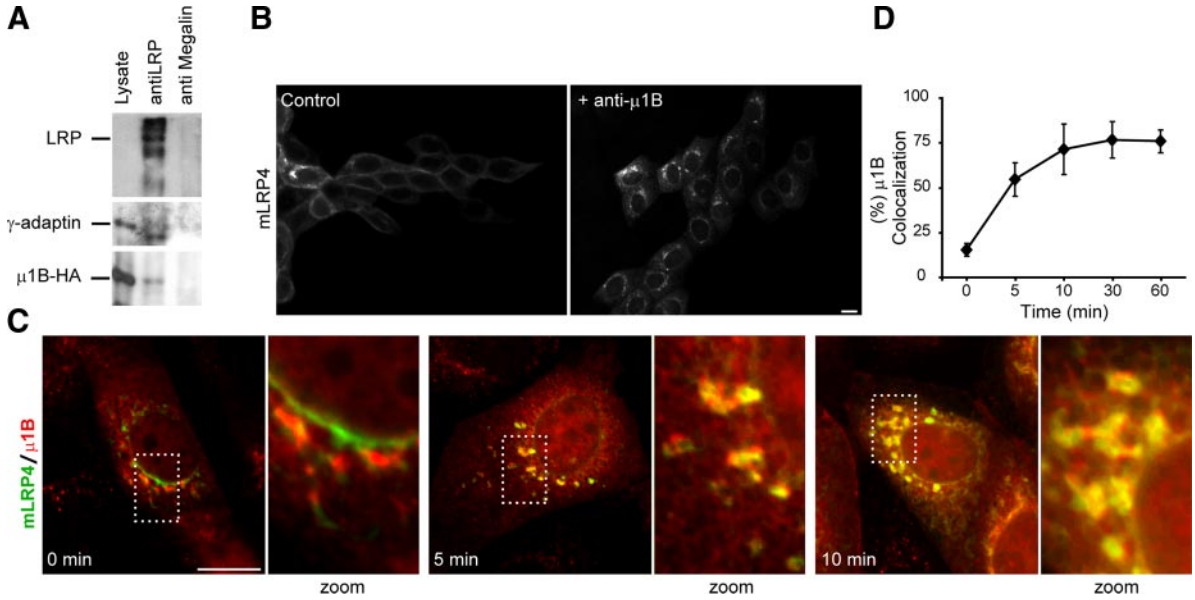

Figure 2. Physical and functional interaction between LRP1 and AP-1B. (A) MDCK cells were transiently transfected with a plasmid encoding μ1B-HA. Cells were lysed and the lysates were immunoprecipitated with anti-LRP1 or anti-megalin antibodies. The immunoprecipitates were resolved on 4–15% SDS-PAGE. The presence of LRP1 was detected by immunoblotting with anti-LRP antibody, and the complex AP-1B was evidenced by the presence of γ-adaptin and μ1-B. (B) FRT cells were microinjected with mLRP4 minireceptor plus RAP cDNAs with or without blocking-function anti-μ1B antibody. Cells were maintained for 1 h at 37°C, followed by 2 h at 20°C to accumulate the receptor at the TGN. After 1 h of exit at 37°C cells were fixed and processed for immunofluorescence with anti-HA to detect the minireceptor. After 60 min, release from TGN block mLRP4 was located on surface in control cells. In contrast, in μ1B-microinjected cells, mLRP4 was located mainly in a perinuclear localization, most likely RE, indicating that AP1B adaptor complex is involved in the intracellular trafficking of the receptor. (C and D) Kinetic analyses of mLRP4/μ1B colocalization of newly synthesized mLRP4 demonstrates that perinuclear accumulation was achieved during biosynthetic trafficking. Scale bar, 10 μm.

wild-type or mutant receptor was expressed together with the chaperone RAP, which is required for correct folding and subsequent transport of LRP1 out of the endoplasmic reticulum (Bu and Marzolo, 2000). In addition, we coexpressed a dominant negative form of the accessory protein eps15 (D/N-eps15), known to interfere with the clathrin-mediated endocytosis of the TfR, as a fusion protein with green fluorescent protein (GFP; Benmerah *et al.*, 1999) and also previously used to block the endocytosis of ApoER2, another member of the LDLR family (Cuitino *et al.*, 2005). We checked that this D/N-eps15 effectively interrupts the internalization of mLRP4wt in transient transfection conditions (Supplemental Figure S2, A and B) and also under the microinjection conditions used, in this case for the mLRP4 $Y_{29}A$ (Supplemental Figure S2C). In this way, we attempted to inhibit the rapid endocytosis of mLRP4 from the basolateral membrane and thus increase the probability of its detection at the cell surface. In addition, this strategy allow us to determine whether the apical distribution of the $Y_{29}A$ receptor mutant derives from a sorting defect at the TGN, resulting in its direct segregation to the apical domain, or at an endosomal compartment, which would determine basolateral to apical transcytosis instead of basolateral recycling.

The cells microinjected with the corresponding plasmids were first incubated for 1 h at 37°C to allow expression and then for 2 h at 20°C to accumulate the newly synthesized proteins at the TGN. After releasing the TGN block for 1 h at 37°C, both the wild-type mLRP4 and the $Y_{29}A$ minireceptor showed a predominant intracellular vesicular pattern, with some apical distribution of $Y_{29}A$ (Supplemental Figure S3). Then, in the presence of D/N-eps15, mLRP4 distributed basolaterally, indicating that its endocytosis was effectively reduced (Figure 5). Instead, in these conditions the $Y_{29}A$ mutant showed an apical cell surface distribution, albeit with some intracellular staining. Supplemental Figure S4 shows higher magnification images corresponding to the same confocal plane, for mLRP4$Y_{29}A$, mLRP4wt and E-cadherin, which clearly illustrate the basolateral distribution of wt minireceptor (coincident with E-cadherin distribution), whereas the mutant was mostly intracellular. These results are representative of the analysis of several fields, quantifying the distribution of minireceptors in 200 microinjected cells (D/N-eps15-GFP–positive cells) per condition (Supplemental Figure S5A). The wild-type receptor distributed basolaterally in about 70% of microinjected cells. In 25% of the cells we could detect apical staining, representing just 7.4% of the total fluorescence (Supplemental Figure S5B), suggesting missorting by overexpression. In contrast, the $Y_{29}A$ mutant distributed apically in 70% of cells, accounting for 50% of the total fluorescence (Supplemental Figure S5B), with the remaining fluorescence being only intracellular.

These results discard two possibilities: First, that the $Y_{29}A$ mutant is sorted without polarity to both cell surfaces and upon endocytosis from the basolateral domain becomes intracellularly arrested at endosomal compartments and subsequently disappears from this domain, and second, that the $Y_{29}A$ mutant reaches the apical pole by transcytosis after rapid endocytosis from the basolateral domain. In both cases, the endocytic inhibition caused by coexpressing D/N-eps15 would have increased the basolateral location of the mutant. The $Y_{29}A$ mutation most likely released otherwise recessive apical sorting information present in the ectodomain (Marzolo *et al.*, 2003).

Experiments in FRT cells showed that after releasing the TGN block in the presence of the function blocking anti-μ1B

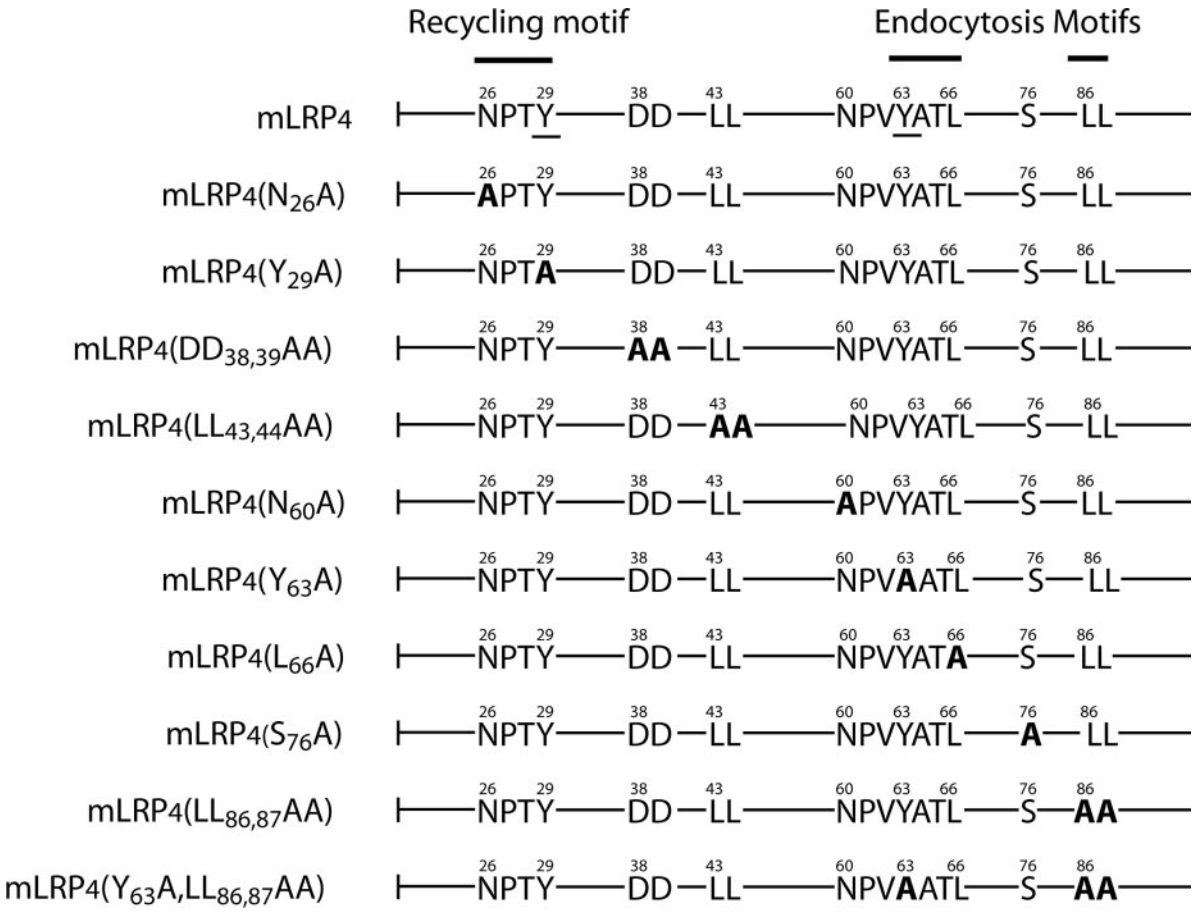

Figure 3. Schematic representation of mLRPs with the potential cytoplasmic basolateral sorting signals and their mutations. The sequence of the wild-type tail (mLRP4) is depicted with the already known recycling and endocytic-sorting motifs described in nonpolarized cells (Li *et al.*, 2000; van Kerkhof *et al.*, 2005) and the two tyrosines (Y_{29} and Y_{63}, underlined) involved in basolateral distribution (Marzolo *et al.*, 2003). All the mutants made are highlighted in bold where the critical residues were replaced by alanine.

antibody the Y_{29}A mutant did not accumulate in the post-Golgi RE (Figure 6), contrasting with the wild-type receptor (see Figure 2). Under these conditions, the Y_{29}A mutant distributed in peripheral vesicles and was not detected at any moment in μ1B-RE, indicating that it was very likely missorted directly from the TGN. Therefore, the Y_{29} seems to be part of a dominant basolateral sorting signal that operates in the TGN during biosynthetic trafficking. The results cannot exclude the possibility that the same sorting signal also operates at RE during post-TGN trafficking or that additional biosynthetic basolateral sorting signals decoded by AP1B direct LRP1 to the basolateral plasma membrane.

The $N_{26}PTY_{29}$ Motif Is Involved in Basolateral Recycling and in Recruiting SNX17 to BSEs

It is currently believed that the functional integrity of NPxY motifs depend equally on both the N and the Y residues (Bansal and Gierasch, 1981). Mutational analysis has revealed that the Y residue can be engaged in functions different from those of the NPxY motif. This was first demonstrated in the LDLR, in which the NPxY motif also acts as an endocytic signal, but the Y residue participates independently of the N residue in basolateral sorting (Matter *et al.*, 1992).

In LRP1, the proximal NPxY motif has no role in endocytosis (Li *et al.*, 2000) but regulates receptor's recycling (van

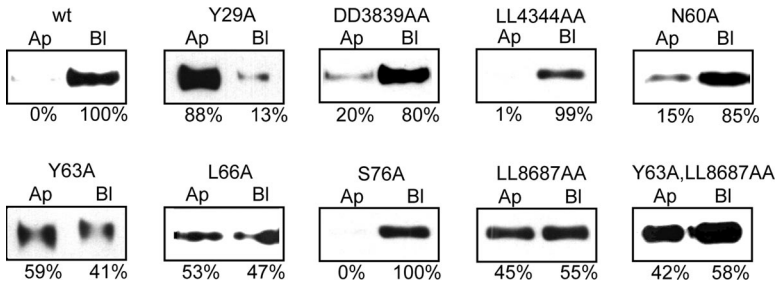

Figure 4. Changes in the steady-state distribution of mLRP4 mutants uncover the critical basolateral sorting motifs within the LRP1 tail. MDCK cells stably expressing the different mLRP4 constructs were grown on filters to determine the membrane distribution of the receptors by domain-specific biotinylation. Biotinylated minireceptors were precipitated with streptavidin-agarose and resolved in 6% SDS-PAGE followed by immunoblot with monoclonal anti-HA. The receptor's relative expression level in each membrane domain was estimated by densitometry of the resulting bands. The critical basolateral determinants include the Y_{29} of the proximal NPxY, the $Y_{63}ATL_{66}$, and the distal $LL_{86,87}$ motifs. Similar results were obtained from two to three clones of each construct.

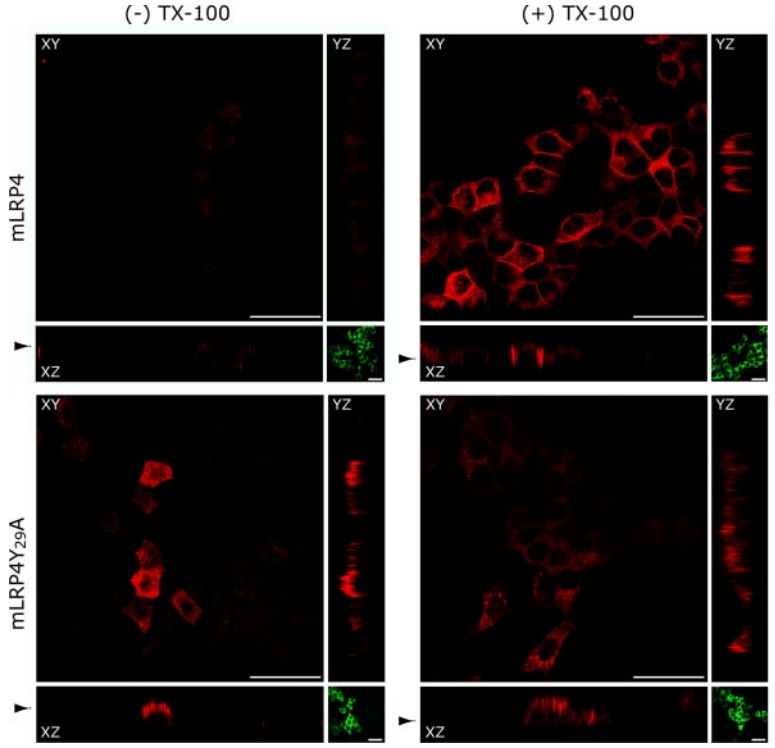

Figure 5. The mLRP4Y_{29}A mutant is directly addressed to the apical domain in MDCK cells. Three days after reaching confluency, MDCK cells plated on glass coverslips were microinjected in the nucleus with the expression plasmids mLRP4 or Y_{29}A together with pcDNA-RAP and a plasmid encoding the dominant negative form of eps15 (D/N-eps15), GFP- Eps15 DD (EΔ95/295). After incubating the cells for 1 h at 37°C, the newly synthesized receptors were accumulated in the TGN at 20°C for 2 h in the presence of cycloheximide. TGN-to-cell-surface protein traffic was then allowed to proceed at 37°C for 60 min, and the cells were treated for indirect immunofluorescence. The apical or intracellular/basolateral surface distributions of the receptors were assessed in nonpermeabilized and permeabilized cells, respectively. Expression of the D/N-eps15 increased mLRP4wt detection at the cell surface. The cells were analyzed by confocal microscopy and representative x-y plane and x-z and y-z sections are shown (red). D/N-eps15 expression is shown in the x-y plane, medial to x-z sectioning (green). The mLRP4wt appears in intracellular vesicles and in the basolateral membrane, whereas the Y_{29}A mutant was present only in intracellular vesicles and at the apical surface, indicating direct TGN-to-apical addressing. Scale bar: 20 μm. Arrowhead indicates selected x-y plane of x-z sectioning.

Kerkhof *et al.*, 2005). Because the Y_{29}A mutation caused missorting to the apical domain, we decided to study the effect an N_{26} A mutation. Surprisingly, in FRT cells, most of the mLRP4N_{26}A mutant displayed an intracellular location instead of an apical distribution (Figure 7A). MDCK cells showed the same effect (not shown). Biotinylation assays could not detect mLRP4N_{26}A mutant at the cell surface of MDCK cells, whereas a rather small amount appeared basolaterally in FRT cells, relative to its total level of expression (Figure 7B). By detecting E-cadherin and Na^+K^+ ATPase at the basolateral domain of MDCK and FRT cells, respectively, we ensured that the cells were correctly polarized and that the biotin had access to the basolateral cell surface.

In a complementary approach, we used flow cytometry to compare the expression level of the wild-type and mutant receptors at the cell surface of MDCK cells. Only 4% of the total mLRP4N_{26}A was at the cell surface, compared with ~33% of the wild-type minireceptor, indicating the mutant minireceptor is able to get the cell surface but with an almost 10-fold less efficiency than mLRP4 wild type (Figure 7C). Thus, our results suggest that after rapid internalization the N_{26}A mutant stays longer in rate-limiting recycling compartments. If this is so, one might expect that inhibiting the LRP1 endocytosis would increase the detection of the mutant at the basolateral cell surface. The microinjection protocol, detailed in Figure 5, to coexpress D/N-eps15 allowed detecting the N_{26}A mutant at the basolateral membrane, albeit in a few cells (Figure 8A). As shown for the wild-type and Y_{29}A mutant minireceptors, we quantified the % of microinjected cells expressing the N_{26}A mutant at the cell surface, finding that no more than 5% of the cells had surface staining, being almost all basolateral (Supplemental Figure S5).

To test directly whether recycling of the N_{26}A mutant is defective in polarized epithelial cells, as was previously

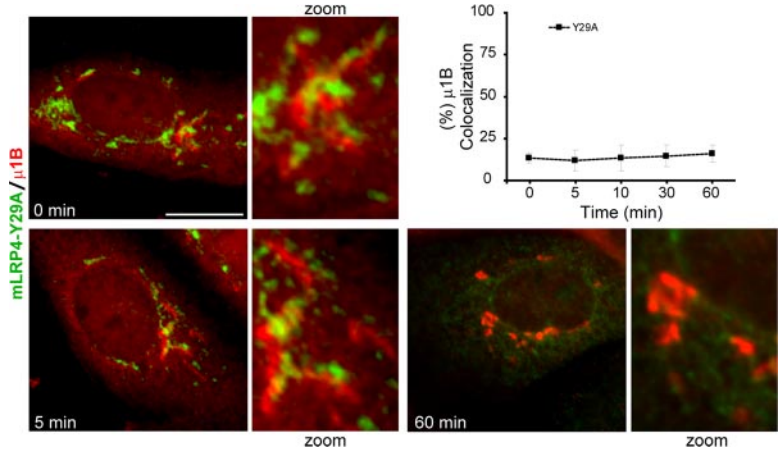

Figure 6. The mutant Y29A does not traffic through post-Golgi compartment to get the apical plasma membrane. FRT cells were microinjected with mLRP4-Y29A minireceptor plus the chaperone RAP cDNAs and the blocking-function anti-μ1B antibody. Cells were maintained for 1 h at 37°C, followed by 2 h at 20°C to accumulate the receptor at the TGN, and then the cells were fixed at the indicated time and processed for immunofluorescence with anti-HA to detect the minireceptor. Kinetic analyses of mLRP4-Y29A/μ1B colocalization of newly synthesized mLRP4-Y29A show that the μ1B compartment is not involved in biosynthetic trafficking of this mutant. Scale bar, 10 μm.

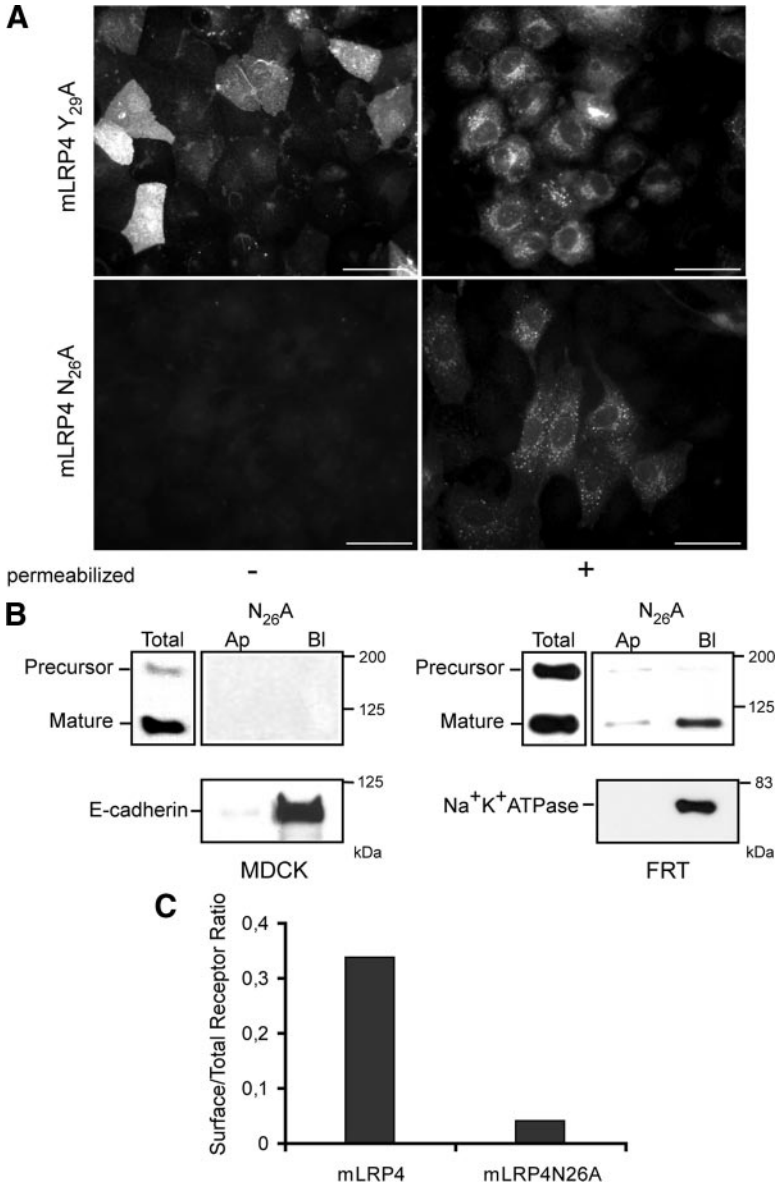

Figure 7. Mutations within the proximal NPxY motif of the LRP1 tail result in different receptor distributions. (A) FRT cells stably transfected with either mLRP4Y_{29}A or mLRP4N_{26}A were grown to confluence on coverslips and treated for indirect immunofluorescence with anti-HA under nonpermeabilized and permeabilized conditions, as indicated. Y_{29}A distributed both at the apical cell surface (right panel) and intracellular vesicles (left panel), whereas N_{26}A show only an intracellular localization, not being detectable at the cell surface. MDCK cells gave similar results (not shown). Scale bars, 10 μm. (B) Domain-specific cell surface biotinylation of MDCK and FRT cells expressing mLRP4N_{26}A. In MDCK cells the protein was not detected at the cell surface. Controls confirmed the receptor expression (immunoblot of total lysate) and proper basolateral expression of E-cadherin. In FRT cells, however, a low amount of minireceptor was detected at the basolateral cell surface. Na^+K^+ ATPase was used as an endogenous basolateral marker. (C) MDCK cells expressing either mLRP4wt or the N_{26}A mutant were consecutively incubated, either intact or after permeabilization with 0.1% saponin with an anti-HA and anti-mouse RPE-conjugated antibody, and analyzed by flow cytometry. The ratio of expression levels observed in intact versus permeabilized cells show 30% of the wild-type receptor versus no more than 4% of the N_{26}A mutant at the cell surface.

shown in nonpolarized cells (van Kerkhof *et al.*, 2005), we used a described cell surface fluorescence quenching recycling assay (van Kerkhof *et al.*, 2005). In this procedure, the receptor that becomes exposed to the cell surface binds Alexa488-labeled anti-HA and after 20 min of internalization, the fluorescent antibody is quenched by an anti-Alexa488 antibody; the magnitude of the quenching being proportional to the receptor's recycling rate. Accordingly to the difference in the cell surface expression of the minireceptors (Figure 7C and Supplemental Figure S5), cells expressing the wild-type protein show a fivefold increase in the total fluorescence intensity compared with the N_{26}A mutant after 20 min of anti-HA internalization (not shown). At 5 min of antibody quenching, the measured recycling efficiency of cells expressing the wild-type mLRP4 was around 27%, compared with <2% for cells expressing the N_{26}A mutant. After 20 min of quenching, the efficiency of recycling for the mutant was still very low (7% compared with 26% of the control).

Taken together, all these results demonstrate that recycling of the mutant N_{26}A receptor is severely impaired (Figure 8B) and more dramatically than in nonpolarized cells (van Kerkhof *et al.*, 2005). Thus the lack of surface localization of this mutant at the steady state is most likely due to abrogation of a motif that promotes recycling.

To determine the sorting compartment where the N_{26}A mutant minireceptor is intracellularly arrested and its relationship with SNX17, a cytosolic protein involved in LRP1 recycling (van Kerkhof *et al.*, 2005), we performed quantitative analysis of immunofluorescent colocalization with the EEA1, an early endosomal marker. We found a significantly increased colocalization of the N_{26}A mutant minireceptor with EEA1 (62 $\pm$ 2.7% of the N_{26}A mutant vs. 54 $\pm$ 2.8% of the mLRP4 wild-type; $p < 0.05$, unpaired *t* test; Figure 9). Because the proximal NPxY is the motif that binds SNX17 and mediates LRP1's recycling (van Kerkhof *et al.*, 2005), we assessed the distribution of SNX17 in cells expressing either the wild-type or the N_{26}A mutant receptor. The two available antibodies recog-

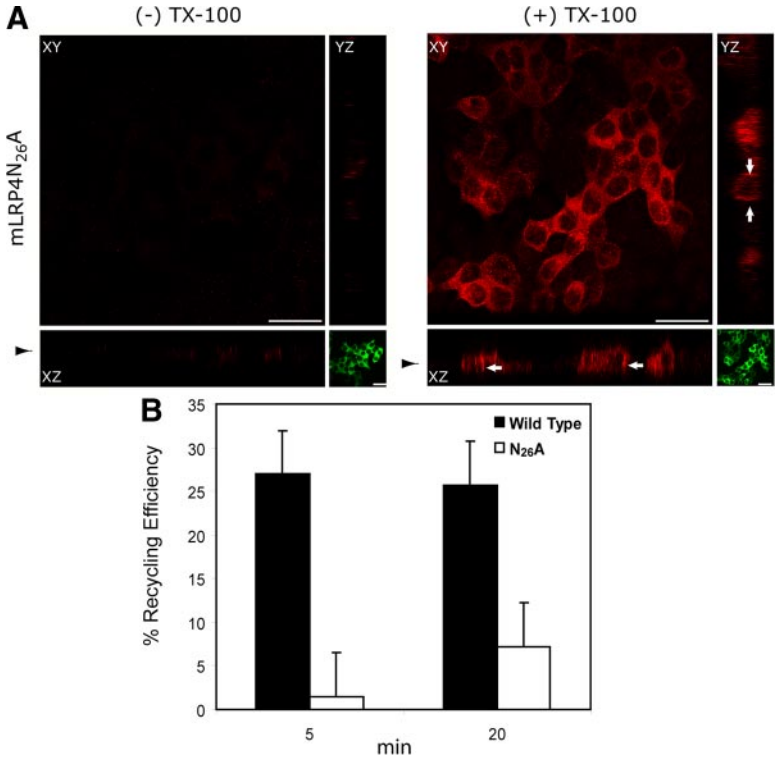

Figure 8. The mutant $N_{26}A$ reaches the basolateral membrane, but its recycling efficiency is severely impaired. (A) MDCK cells were microinjected 3 d after reaching confluence with the plasmid encoding the D/N-eps15, GFP- EPS15 DD (EΔ95/295) as described and analyzed in Figure 5. Confocal microscopy and representative x-y plane and x-z and y-z sections are shown (red). D/N-eps15 expression is shown as x-y plane medial of x-z sectioning (green). The distribution of the $N_{26}A$ mutant was mainly intracellular, but was also detectable at the basolateral membrane (arrows). Scale bar, 20 μm. Arrowhead indicates selected x-y plane of x-z sectioning. (B) The recycling efficiency of the minireceptors was evaluated in MDCK cell lines by a fluorescence quenching assay. The mLRP4wt or $N_{26}A$ mutant were labeled with Alexa488-conjugated anti-HA antibody at 37°C for 20 min and then chased for the indicated time periods in the presence of quenching anti-Alexa488 IgG. Cells were processed for flow cytometry, and the recycling efficiency was calculated. The data were plotted and are shown in the graph, corresponding to two experiments measured in duplicate. Average values are shown; error bars, SEM.

nizing the human protein (van Kerkhof *et al.*, 2005) detect the endogenous SNX17 in MDCK cells in immunoblot (not shown), but not by immunofluorescence. Therefore we performed microinjection experiments to express myc-tagged human SNX17 together with the minireceptors and RAP.

Interestingly, SNX17 displayed a better endosomal distribution when coexpressed with the wild-type minireceptor than with the $N_{26}A$ mutant receptor. In cells expressing the mLRP4wt 37 ± 3.3% of EEA1 endosomes contained SNX17, versus 5.8 ± 1.8% in cells expressing the $N_{26}A$ mutant. The wild-type minireceptor colocalized 33 ± 3% with vesicular SNX17, versus 7 ± 2.1% by the $N_{26}A$ mutant receptor. These results show that mLRP4 promotes SNX17 recruitment to EEA1 early endosomes and provide further evidence that N_{26} is part of a sorting signal that mediates LRP1 basolateral recycling. As judged by the immunofluorescence patterns, the rate-limiting step of LRP1 recycling could be EEA1/SNX17 containing compartments.

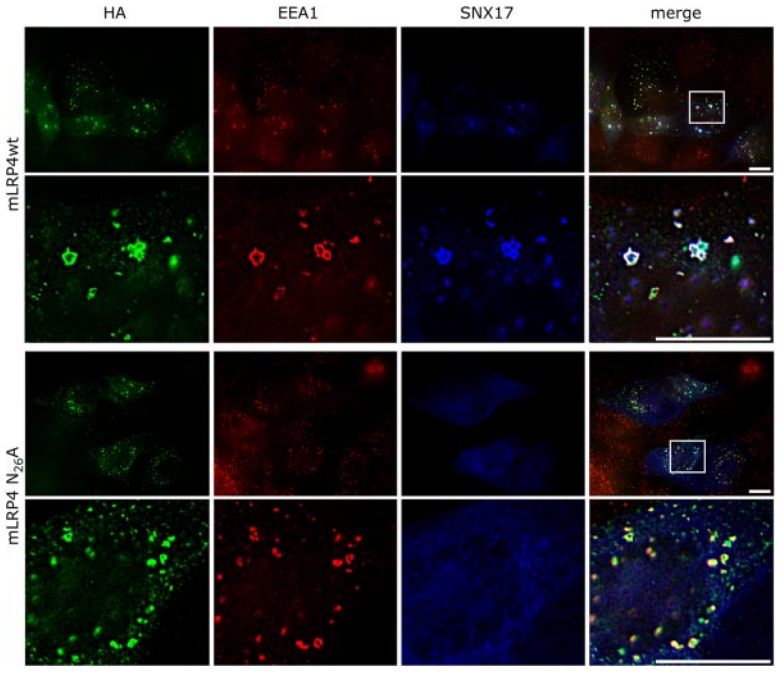

Figure 9. Colocalization of minireceptors with endosomal markers EEA1 and SNX17. MDCK cells were microinjected with the plasmids encoding for RAP, SNX17-myc, and either the mLRP4wt or $N_{26}A$ minireceptors. Cells were processed for immunofluorescence to detect the HA-tagged minireceptor (green), the early endosome marker EEA1 (red), and the myc-tagged SNX17 (blue). In the amplified merged images, colocalization of the wild-type minireceptor with EEA1 in endosome-like structures was clearly visible; some of these structures also contain SNX17 (white dots). The $N_{26}A$ minireceptors practically did not colocalize with SNX17 and exhibited an increased colocalization with EEA1 (amplified merge image, yellow dots). Scale bars, 10 μm.

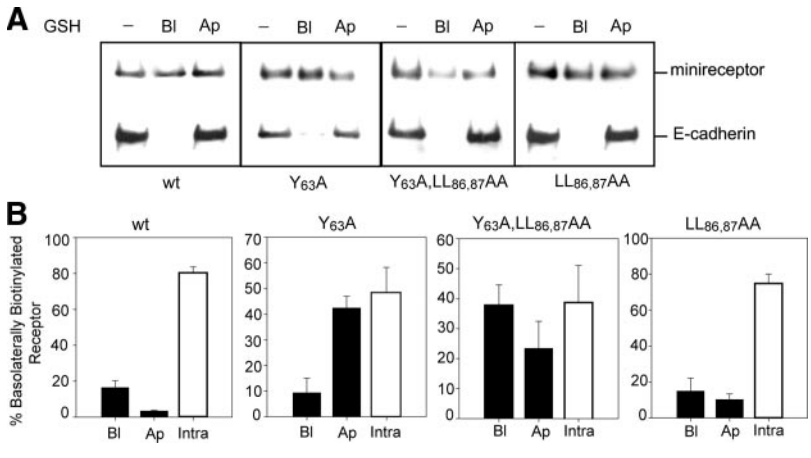

Figure 10. Basolateral to apical transcytosis of mLRPs in MDCK cells. MDCK cells stably expressing one of the following constructs: mLRP4wt, mLRP4$LL_{86,87AA}$, mLRP$Y_{63}A$, or the double mutant minireceptor, were grown on filters to confluence. Cells were biotinylated with reducible biotin at 4°C, shifted to 37°C for 45 min, and reduced with glutathione either at the apical or basolateral surface. Cells were lysed, biotinylated proteins were precipitated with streptavidin beads, and the complexes resolved by reducing 6% SDS-PAGE and Western blot. (A) Minireceptor detection with anti-HA and E-cadherin blot. The absence of apical reduction of biotinylated E-cadherin indicates that the observed reduction of the minireceptor was due to its transcytosis from the basolateral to the apical surface. (B) Bands were quantified, and the total biotinylated minireceptor was taken as 100% (see *Material and Methods*). Minireceptor present in the basolateral surface, apical surface and within the cells was determined as a percentage of total. The determinations were performed in triplicate for each construct.

All these results indicate that N_{26} and Y_{29} residues conform distinct sorting determinants that act at different steps of LRP1 trafficking. The Y_{29} constitutes a biosynthetically basolateral sorting signal that functions at the TGN, and acts independently of the NPxY motif, whereas the N_{26} and the Y_{29} residues within the proximal NPxY motif regulate an additional sorting event occurring at the recycling route of the receptor. This recycling step most likely involves SNX17 recruitment to the EEA1 endosomes that would represent an earlier compartment than μ1B-containing endosomes.

The Endocytic Motifs, Y_{63}ATL and $LL_{86,87}$, Also Contribute to Receptor Basolateral Recycling

The nonpolarized cell surface distribution of LRP1 mutants $Y_{63}A$ and $LL_{86,87A}$ resemble LRP1 in the absence of AP1B (Marzolo *et al.,* 2003), thus suggesting that these motifs are involved in basolateral sorting from a μ1B recycling compartment. Indeed, μ1B could recognize tyrosine-based motifs of the kind of $Y_{63}ATL_{66}$. In addition, both $Y_{63}A$ and $LL_{86,87A}$ motifs have been reported to decrease, but not completely abrogate, the endocytic rate of LRP1 (Li *et al.,* 2000). Therefore, these motifs could also contribute to the polarized recycling, maybe at a different step than that mediated by $N_{26}PxY_{29}$ motif. To test this hypothesis, we performed transcytosis assays in MDCK cells grown on filters, using glutathione stripping of cleavable sulfo-NHS-SS-biotin (Figure 10). After basolateral biotinylation the cells were incubated for 45 min at 37°C. The majority (80 ± 5%) of the mLRP4 wild-type becomes insensitive to glutathione stripping from the apical or basolateral cell surfaces, indicating internalization and steady-state distribution at intracellular compartments, with almost undetectable transcytosis (3.3 ± 0.3%). On the contrary, a percentage of the basolaterally biotinylated mutants, 42.4 ± 4.6% of the $Y_{63}A$, 24 ± 6% of double mutant $Y_{63}A/LL_{86,87AA}$, and 11 ± 3% of $LL_{86,87}AA$ mutants, became sensitive to glutathione stripping from the apical cell surface, reflecting an increased basolateral-to-apical transcytosis. These results indicate that Y_{63} and the $LL_{86,87}$ promote basolateral recycling, in addition to internalization of LRP1. Disruption of these residues causes nonpolarized recycling, a fraction to the basolateral surface and a fraction to the opposite domain by transcytosis.

The lack of colocalization of SNX17 and μ1B in polarized MDCK cells (Supplemental Figure S6) strongly suggests that LRP1 experiences two postendocytic recycling steps spatially and temporally separated. The dominant recycling step would depend on the proximal NPxY motif and SNX17 operating at the basolateral sorting endosome (BSE), whereas the few receptors that escape this sorting event would enter into the μ1B-RE and rescued to a basolateral sorting.

Neurons Decode LRP1-sorting Motifs with Mechanisms Similar to Those in Epithelial Cells

LRP1 has been localized in the somatodendritic domain (Brown *et al.,* 1997), but the sorting elements that determine this distribution remain unknown. Having defined the effect of our LRP1 mutants in polarized epithelial cells and the role of μ1B and SNX17 in LRP1 basolateral sorting, we went on to assess their sorting behavior in neurons that are known to lack AP1B (Ohno *et al.,* 1999).

We transfected primary cultured hippocampal neurons with each of the mLRP4 constructs and, by indirect immunofluorescence with anti-HA monoclonal antibodies, assessed the cell surface distribution of the minireceptor in nonpermeabilized cells. Then, we permeabilized the cells to define the somatodendritic domain by MAP2 staining (Caceres *et al.,* 1984). As expected for a somatodendritic protein, the wild-type minireceptor mLRP4 completely colocalized with MAP2 (Figure 11). Minireceptors with $Y_{63}A$ and $LL_{86,87AA}$ mutations mimicked epithelial-sorting behavior when expressed in neurons. Both distributed without polarity, evenly in somatodendritic and axonal domains. Strikingly, the $Y_{29}A$ mutant distributed exclusively at the distal part of the axon.

In permeabilized neurons, the wild-type minireceptor exhibits an exclusively somato-dendritic vesicular distribution (Figure 12), resembling the TfR that is also excluded from the axon (Cameron *et al.,* 1991). The intracellular vesicles carrying the $Y_{29}A$ mutant, however, distributed both in axons and dendrites. The mechanistic relationship between such intracellular nonpolarized distribution and the distal axonal sorting that this mutant displays at the cell surface remains unknown.

The sorting behavior of the $N_{26}A$ mutant was similar to that as seen in MDCK cells. We could not detect the minireceptor mLRP4$N_{26}A$ at the cell surface of nonpermeabilized neurons, whereas permeabilized cells show intense immunofluorescence staining, indicating intracellular accumulation (Figure 13A). These results suggest that in hippocampal neurons, LRP1 also recycles through a mechanism

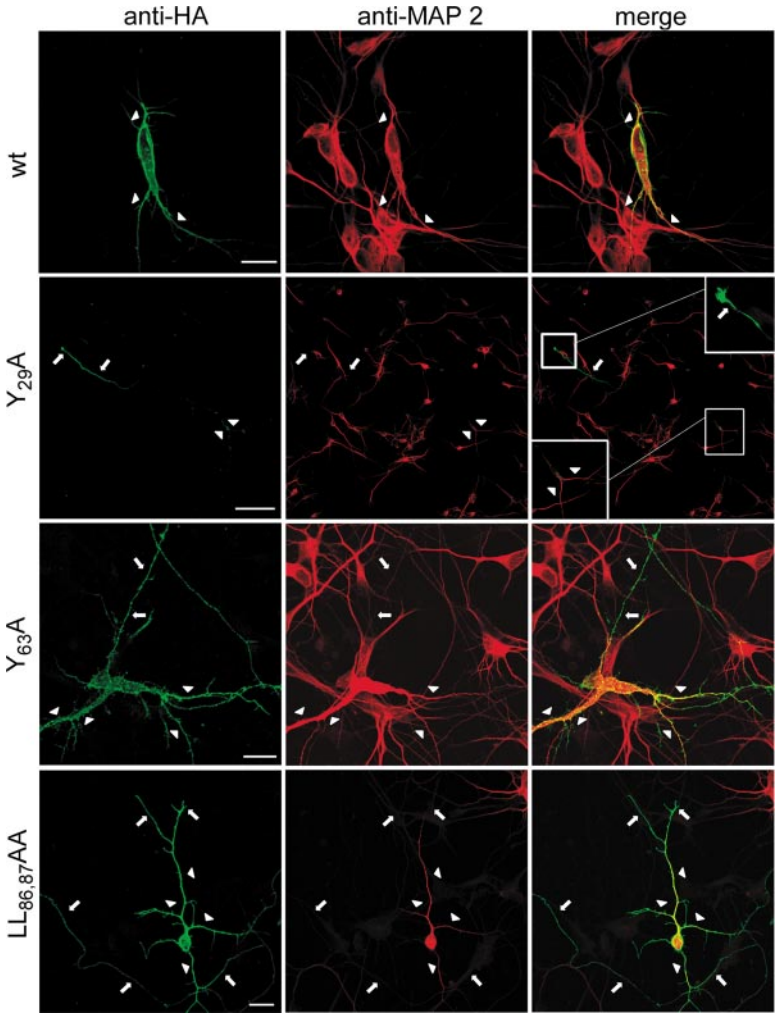

Figure 11. The somatodendritic distribution of mLRP in hippocampal neurons depends on the same motifs required for its basolateral distribution in epithelial cells. Primary cultured hippocampal neurons were transfected as described in *Materials and Methods*. The distribution of the transfected mLRP was determined by confocal microscopy, using anti-HA to detect the receptor at the cell surface (green) and, after cell permeabilization, using anti-MAP2 (red) to determine the somatodendritic domain. The restricted cell surface somatodendritic distribution of mLRP (arrowheads) was lost when the critical basolateral determinants, based on tyrosines and dileucines, were replaced by alanines. This was visualized by the axonal staining of the receptor in MAP2-negative structures (arrows). The most striking distribution was the mLRP$Y_{29}A$ mutant, for which only the distal region of the axon was positively stained with anti-HA. Scale bars, 20 μm (wt, $Y_{63}A$ and $LL_{86,87AA}$) and 100 μm ($Y_{29}A$).

that depends on the $N_{26}PxY_{29}$ motif. Supporting this possibility, SNX17 is shown to be endogenously expressed in cultured hippocampal and cortical neurons (Figure 13B).

All these results suggest that the same sorting motifs that address LRP1 basolaterally in epithelial cells operate to somatodendritically target the receptor in neurons, de-

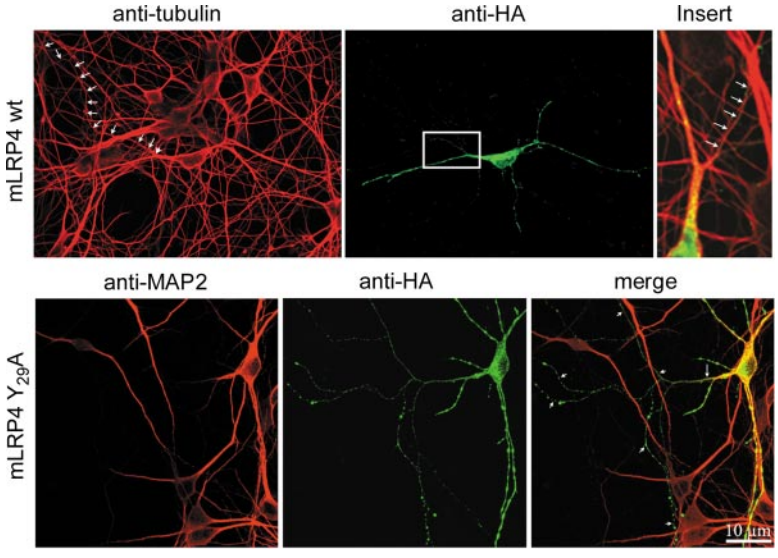

Figure 12. Intraneuronal distribution and unrestricted transport of the mLRP4$Y_{29}A$ mutant to the axons. Top, confocal micrographs showing the distribution of tubulin (red) and HA-tagged mLRP4wt (green) in 7 DIV (days in vitro) permeabilized cultured hippocampal neurons. HA-tagged mLRP4 localized to short, dendritic-like processes. Note that a thin long axon-like neurite (arrows) that emerges from a dendritic shaft (arrowhead) and that is positive for tubulin does not contain HA-tagged mLRP4. The inset on the right panel (merge color) shows a high-magnification view of the region where the axon-like neurite originates. Bottom, confocal micrographs showing the distribution of the somatodendritic marker MAP2 (red) and the mutant HA-tagged mLRP4$Y_{29}A$ (green) in 7 DIV cultured hippocampal neurons. Note that the ectopic mutant variant of mLRP4 not only localized to dendritic-like processes, but also to MAP2 (−), axon-like neurites (short arrows in the merge panel). The long arrow in the merge panel shows the dendritic site from which the axon merges. For these experiments cells were fixed and permeabilized 18 h after transfection. Scale bar, 10 μm.

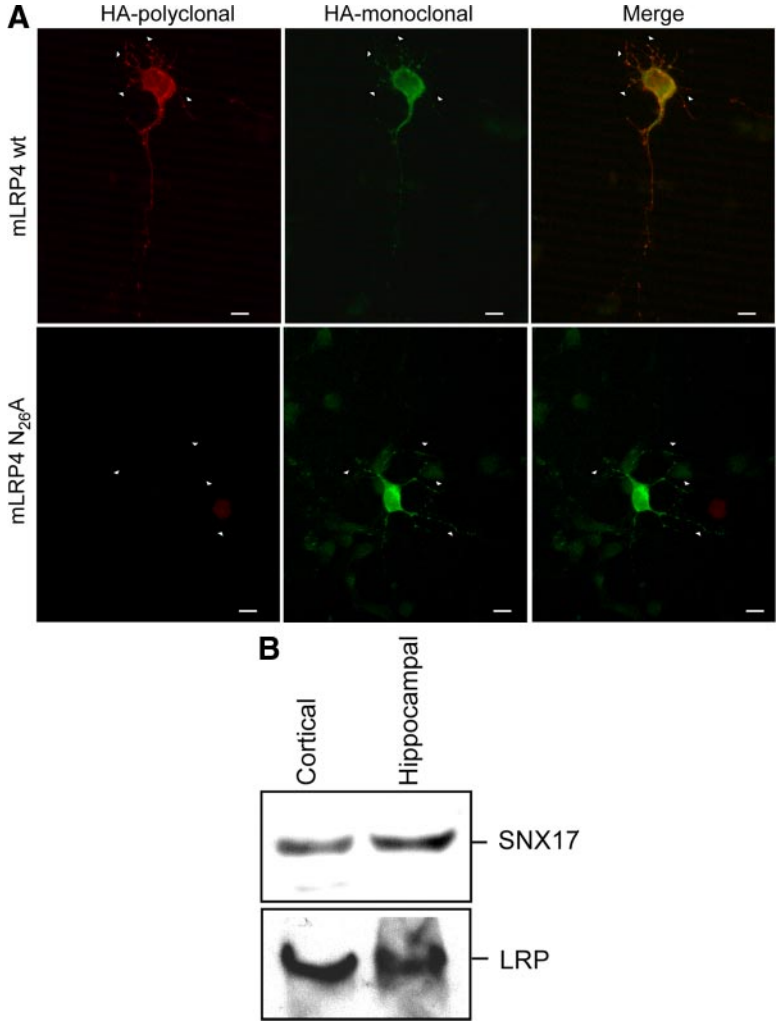

Figure 13. Intraneuronal distribution and absence of cell surface expression of the mLRP4N_{26}A mutant in hippocampal neurons. (A) Differential cell surface expression of mLRP4wt (top panel) and N_{26}A (bottom panel) in hippocampal neurons in primary culture was evidenced by immunofluorescence detection of the surface minireceptor using a polyclonal anti-HA (red), followed by permeabilization and detection of the intracellular minireceptor using a monoclonal anti-HA (green). The wild-type mLRP4 was expressed in the somato-dendritic surface, but the N_{26}A mutant was only intracellular and somatodendritic. Scale bars, 10 μm. (B) Hippocampal neurons cultured 7 d in vitro and cortical neurons were lysed, 100 μg of proteins were resolved in reducing SDS-PAGE, and the presence of endogenous SNX17 and LRP1 was determined by Western blot.

spite the differences in the expression of AP1B. In this system the recycling step would be only mediated by SNX17.

DISCUSSION

This work shows novel features of the sorting mechanisms involved in the polarized distribution of LRP1, by defining the trafficking behavior of sorting mutants and the participation of AP1B and SNX17. The biosynthetic basolateral pathway of LRP1 includes a TGN sorting event, mediated by Y_{29}, and a post-TGN trafficking through μ1B-containing RE, which is blocked by an μ1B antibody (Cancino *et al.*, 2007). Y_{29}A mutants were apically missorted without entering this μ1B-RE, indicating that Y_{29} directs LRP1 from TGN to RE. We also detected an interaction of LRP1 with AP1B by coimmunoprecipitation, in agreement with our previous observation of LRP1 missorting in cells lacking μ1B (Marzolo *et al.*, 2003). We also found that a different Y-dependent sorting signal mediates LRP1 basolateral recycling, implicating distinct sorting elements operating during biosynthetic and recycling trafficking. These sorting elements include, for the first time, SNX17 recruitment to BSEs, which are distinct from the AP1B endosomes. Finally, sorting signals of LRP1 seem to be similarly decoded in neurons. We found that neurons, which lack AP1B, express SNX17 and the LRP1 mutant with a defective SNX17-binding site distributes intracellularly as expected for a recycling defect. This suggests that SNX17 constitutes a conserved element of the polarized protein-sorting machinery between neurons and epithelial cells.

Mutational analysis revealed multiple motifs contributing to basolateral distribution of LRP1, including Y_{29}, N_{26}, Y_{63}, and $LL_{85,86}$ residues. The individual silencing of these residues produces distinct LRP1 distribution patterns, indicating that they are not functionally redundant and cannot compensate the lack of each other. The different phenotypes could be explained by temporal-spatial differences in the sorting events that these motifs mediate.

In nonpolarized cells the proximal NPxY motif of LRP1 constitutes both a binding site for SNX17 and a sorting motif for SNX17-mediated receptor recycling (van Kerkhof *et al.*, 2005). The mutant $NPxA_{29}$ showed lower recycling efficiency, and SNX17 knockdown by siRNA inhibited LRP1 recycling (van Kerkhof *et al.*, 2005). Although these studies only analyzed the recycling effect of the Y_{29}A mutant, they show that both Y_{29} and N_{29} residues are required for SNX17 binding in vitro. Therefore, one might expect that both N_{26}A and Y_{29}A mutant receptors display similar sorting defects unless they follow different pathways. Our current results clearly demonstrate that N_{26} and Y_{29} residues exert separable functions at different sorting places in polarized cells.

In polarized cells, the $N_{26}A$ mutation dramatically decreased the cell surface expression of LRP1. The receptor became intracellularly accumulated in endosomes that contain EEA1, thus corresponding to described BSE (Wilson *et al.*, 2000). LRP1 has a very high internalization rate, ~10 times higher than LDLR's (Li *et al.*, 2001a), thus at steady state, it distributes mainly at intracellular endocytic pools, but also basolaterally in small yet detectable levels (Marzolo *et al.*, 2003). In MDCK cells, we performed microinjection experiments to follow the sorting of LRP1 minireceptors from the TGN to the cell surface. Coexpression of D/N-eps15 to inhibit LRP1 endocytosis increased the basolateral distribution of the wild-type minireceptors. However, the distribution of the $N_{26}A$ mutants was much less affected, as expected for a defect in recycling, which was demonstrated using a sensitive recycling assay and cytometry. The results showed that recycling efficiency of $N_{26}A$ mutant decreased by ~90%.

The only proteins so far described to mediate Y-dependent basolateral sorting have been the clathrin adaptors AP4 (Simmen *et al.*, 2002) and AP1B (Folsch *et al.*, 1999; Sugimoto *et al.*, 2002). In nonpolarized cells, LRP1 recycling involves SNX17 (van Kerkhof *et al.*, 2005). Strikingly, we found here that the wild-type minireceptor, but not the $N_{26}A$ mutant, recruits SNX17 to EEA1-containing BSE, the same compartments in which the mutant accumulates. This previously unnoticed correspondence between NPxY-mediated SNX17 endosomal recruitment and LRP1 recycling indicates that SNX17 constitutes a novel element of the basolateral recycling machinery.

When the $Y_{29}A$ mutant was coexpressed with D/N-eps15 and after having exited the TGN, it appeared at the apical cell surface, without displaying any basolateral location. Therefore, in epithelial cells the $Y_{29}A$ mutant does not follow the same pathway as the $N_{26}A$ mutant; otherwise, a recycling arrest would have led to its intracellular accumulation, with very little or undetectable cell surface expression. Experiments performed in FRT cells, which first accumulated the $Y_{29}A$ in the TGN by the 20°C block and then followed its exit from this compartment, did not detect a transit through the μ1B-RE, in contrast to the wild-type receptor. Thus, the data fit better with a scenario in which the $Y_{29}A$ mutant, due to recessive apical information possibly contained in its ectodomain (Marzolo *et al.*, 2003), reaches the apical surface directly from the TGN rather than from the post-Golgi endosomal compartment or from the basolateral cell surface by transcytosis (Figure 14). Thus, LRP1 contains a Y_{29}-dependent, but N_{26}-independent, sorting signal for biosynthetic basolateral sorting at the TGN, whereas the $N_{26}PxY_{29}$ motif directs postendocytic exit from BSE, through a mechanism involving membrane recruitment of SNX17 (Figure 14).

Exhaustive studies on LDLR have led to the prevalent notion that the same Y-dependent basolateral information is decoded during biosynthetic and recycling trafficking (Matter *et al.*, 1993). In this sense, our results constitute the first indication that the biosynthetic and recycling sorting machineries can distinguish between Y-based sorting motifs. Furthermore, we provide evidence that such distinction could be due to temporally and spatially separated sorting events accomplished by yet unknown adaptors at the TGN, AP1B in RE, and SNX17 in BSEs. In FRT cells, where our anti-μ1B antibody is suitable for immunofluorescent staining of endogenous μ1B, we found that the SNX17 endosomes contain EEA1, which is considered a marker of BSEs (Wilson *et al.*, 2000), but do not contain μ1B. AP1B distributes poorly in early endosomes labeled with rab 5 (Gan *et al.*, 2002) and distributes in a compartment with typical characteristics of CRE (Cancino *et al.*, 2007). Because CRE is downstream BSE, all these observations mean that most recycling of LRP1 is SNX17-mediated at BSEs before reaching CRE.

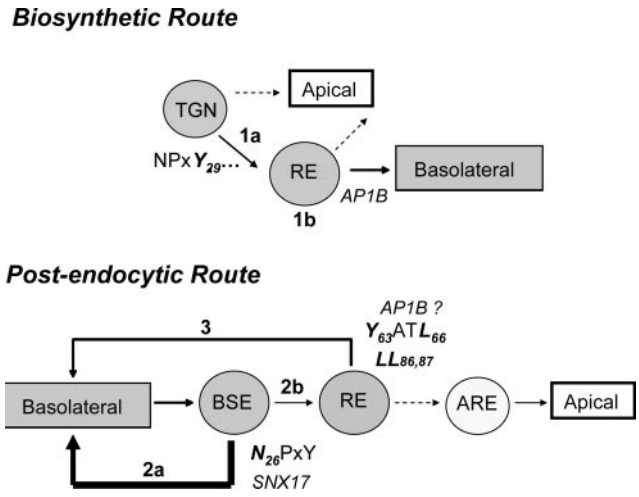

Figure 14. Working model for LRP1 intracellular trafficking in epithelial cells. The data obtained in this work and others previously published (Marzolo *et al.*, 2003; Rodriguez-Boulan *et al.*, 2005; van Kerkhof *et al.*, 2005; Cancino *et al.*, 2007) allow us to derive a working model for LRP1 trafficking. During the biosynthetic pathway, LRP1 is primarily segregated into basolateral-destined vesicles through the recognition of Y_{29}, likely without an NPxY motif. This recognition step occurs at the TGN and likely requires a not yet known adaptor protein(s) that recognizes the critical tyrosine residue (1a). Most of LRP1 should be then segregated by AP1B in the RE (1b), probably recognized through the distal tyrosine-based signal YATL. When the sorting signal is mutated or the corresponding sorting machinery is functionally absent, the receptor fails to be correctly segregated and is directed to the apical membrane or to both domains (punctuate arrow). Once LRP1 arrives at the basolateral membrane, it is actively endocytosed and has to be postendocytically segregated from the basolateral sorting endosome (BSE) in a manner that depends on the proximal NPxY motif and SNX17 (2a; van Kerkhof *et al.*, 2005). A failure in this step causes LRP1 to be trapped in this compartment. After BSE (2b), a secondary recycling step may occur at the common RE and depend on the $Y_{63}ATL_{66}$/$LL_{86,87}$ motifs and probably on the AP1B adaptor complex as well (Marzolo *et al.*, 2003) (3).

Our results reinforce the notion that NPxY motifs can have distinct sorting functions and even dual functions in a same protein depending on the kind of cell. The trafficking role of NPxY motifs of other proteins seems to be mainly endocytic (Chen *et al.*, 1990; Hsu *et al.*, 1994; Cuitino *et al.*, 2005). However, neither of the two cytosolic NPxY motifs of LRP1 play roles in internalization (Li *et al.*, 2000). In the LDLR, the proximal NPxY motif is an endocytic motif in which the tyrosine residue, independent of the N and P residues and together with downstream acidic residues, constitutes a mild basolateral sorting signal, as it is easily overcome by receptor overexpression and becomes apparent only in truncated receptors (Matter *et al.*, 1992, 1994). The strongest basolateral sorting signal of the LDLR depends on a more distal tyrosine and also includes distal acidic residues (Matter *et al.*, 1994). In contrast, the proximal Y_{29}-dependent basolateral sorting signal of LRP1 is rather independent of downstream acidic residues and exerts basolateral destination even upon receptor overexpression and in the context of the entire cytosolic tail, thus acting as a strong basolateral determinant. This Y_{29} residue also belongs to an NPxY motif, but it is only crucial for basolateral recycling. These results show for the first time

that trafficking information embedded within a single NPxY motif can assign distinct temporal-spatial sorting functions to the Y residue.

We previously showed that Y_{63} also exerts a basolateral sorting function (Marzolo *et al.*, 2003). Y_{63} is shared by a distal $N_{60}PxY_{63}$ motif and by the previously identified endocytic motif Y_{63}ATL (Li *et al.*, 2000). Here, we demonstrate that the Y_{63}ATL is a basolateral sorting motif that seems to function in concert with the other LRP1 endocytic signal $LL_{86,87}$ (Li *et al.*, 2000). Disruption of any of these motifs separately or together in a double mutant $Y_{63}A/LL_{86,87AA}$ results in nonpolarized receptor distribution, suggesting that both act as a single complex sorting signal. Furthermore, the sorting information conveyed by Y_{63}ATL and $LL_{86,87}$ does not compensate for the $Y_{29}A$ mutation, thus ruling out their participation at the TGN.

Because $Y_{63}A$ mutant has been shown to decrease but not completely abrogate the endocytic rate of LRP1 (Li *et al.*, 2000), the loss of polarity of this mutant could be achieved during its recycling traffic through a compartment different from BSE, in which the $N_{26}PxY_{29}$/SNX17 system mediates basolateral recycling. Our biotinylation assays demonstrated that these mutants undergo basolateral-to-apical transcytosis. Taken together, the overall results suggest that $Y_{63}A$ mutants are first addressed basolaterally by Y_{29}-dependent sorting at the TGN and then become missorted to both plasma membrane domains when they reach the CRE compartment, presumably after several rounds of recycling from the SNX17-containing BSE. Because the nonpolarized distribution of the endocytosis mutants is similar to the distribution of LRP1 in cells lacking μ1B (Marzolo *et al.*, 2003), the most plausible model is that Y_{63}ATL and $LL_{86,87}$ motifs contribute to AP1B-dependent basolateral sorting of LRP1 in CRE compartment, both during post-TGN biosynthetic trafficking and post-SNX17 recycling trafficking. This model implies that AP1B and SNX17 sort LRP1 at different stations of its endocytic recycling itinerary recognizing distinct sorting motifs (see proposed model in Figure 14).

A matter still under scrutiny and debate is the proposed correspondence between basolateral/apical sorting in epithelial cells and somatodendritic/axonal sorting in neurons (Dotti and Simons, 1990; Silverman *et al.*, 2005). It could be dependent on the specific type of sorting signals possessed by individual proteins. For instance, mutants of the LDLR and TfR lacking basolateral sorting signals are directed apically in MDCK cells but without polarity in neurons (Jareb and Banker, 1998). This suggests that neurons cannot handle recessive apical information contained in these proteins. There is also evidence suggesting that neurons do not recognize dihydrophobic-based basolateral sorting signals (Silverman *et al.*, 2005). However, the sorting behavior of wild type and all our mutant receptors expressed in hippocampal neurons show striking congruency with the sorting correspondence hypothesis. Even the apical $Y_{29}A$ mutant segregate exclusively into the distal part of the axon, whereas the $Y_{63}A$ and $LL_{86,87AA}$ mutants segregate without polarity. This indicates that neurons can effectively decode recessive apical information as well as dihydrophobic somatodendritic sorting signals in recycling proteins. Interestingly, both the axon and dendrites contained intracellular vesicles carrying the $Y_{29}A$ mutant, suggesting a complex mechanism of distal axonal regionalization that, as described for other axonal proteins such as NgCAM (Horton and Ehlers, 2003), might involve selective fusion/retention processes. Neurons do not express AP1B (Ohno *et al.*, 1999), but we found that they do express SNX17. Furthermore, neurons also intracellularly distributed the $N_{26}A$ mutant lacking the SNX17 binding motif. In principle, AP4, which has been involved in somatodendritic addressing of the glutamate-receptor δ2 (Yap *et al.*, 2003), could sort LRP1 at the TGN, whereas SNX17 could play a predominant role in LRP1 somatodendritic recycling. The missorting similarities of the LRP1 mutants suggest conservation of the compartmentalized use of sorting signals at the TGN and recycling compartments in epithelial cells and neurons.

LRP1 is required for development and exerts crucial physiological functions in tissues such as brain, liver and different epithelia, which rely on polarized cells (Herz *et al.*, 1992; Herz *et al.*, 1993). We could anticipate, in accordance with recent data (Roebroek *et al.*, 2006), that natural mutants affecting those critical sorting motifs that we have defined, especially the proximal NPxY, would be relatively unviable.

ACKNOWLEDGMENTS

We thank Dr. Alexander Benmerah (Institut Cochin, U567 INSERM/UMR8104 CNRS, Paris, France) for giving us the plasmid encoding the dominant negative forms of eps15 with GFP and Dr. Ira Mellman (Genentech, South San Francisco, CA) for providing us the cDNA of μ1B-HA-tagged. From the Facultad de Ciencias Biológicas, PUC, we thank Dr. Alejandra Alvarez for providing us some of the hippocampal neurons used in this work, and Dr. Alexis Kalergis and Leandro Carreño for providing access to the FACS equipment. We also thank Dr. María Isabel Yuseff for the characterization of the human anti-EEA1 antibodies in our laboratory and Olivia Ying for reviewing this manuscript. This work was supported by FIRCA grant TW006456 to G.B. and M.P.M., National Institutes of Health Grant R01 AG027924 to G.B., an Alzheimer's Disease Research grant from the American Health Assistance Foundation (AHAF) to G.B., Grant 1020746 from the Fondo Nacional de Investigación Científica y Tecnológica (FONDECYT) to M.P.M., Fondo de Investigación Avanzada en Areas Prioritarias (FONDAP) Grant 13980001 and MIFAB to M.P.M. and A.G. It was also supported by grants from Comisión Nasional de Investigación Cientifico y Technológico (CONICET) and Agencia Nacional de Promoción Científica y Tecnológica (ANPCyT; Argentina) to A.C. G.B. is an Established Investigator of the American Heart Association.

REFERENCES

Ang, A. L., Taguchi, T., Francis, S., Folsch, H., Murrells, L. J., Pypaert, M., Warren, G., and Mellman, I. (2004). Recycling endosomes can serve as intermediates during transport from the Golgi to the plasma membrane of MDCK cells. J. Cell Biol. *167*, 531–543.

Aroeti, B., and Mostov, K. E. (1994). Polarized sorting of the polymeric immunoglobulin receptor in the exocytotic and endocytotic pathways is controlled by the same amino acids. EMBO J. *13*, 2297–2304.

Bacskai, B. J., Xia, M. Q., Strickland, D. K., Rebeck, G. W., and Hyman, B. T. (2000). The endocytic receptor protein LRP also mediates neuronal calcium signaling via N-methyl-D-aspartate receptors. Proc. Natl. Acad. Sci. USA *97*, 11551–11556.

Banker, G. A., and Cowan, W. M. (1977). Rat hippocampal neurons in dispersed cell culture. Brain Res. *126*, 397–425.

Bansal, A., and Gierasch, L. M. (1981). The NPXY internalization signal of the LDL receptor adopts a reverse-turn conformation. Cell *67*, 1195–1201.

Benmerah, A., Bayrou, M., Cerf-Bensussan, N., and Dautry-Varsat, A. (1999). Inhibition of clathrin-coated pit assembly by an Eps15 mutant. J. Cell Sci. *112*, 1303–1311.

Bottenstein, J. E., and Sato, G. H. (1979). Growth of a rat neuroblastoma cell line in serum-free supplemented medium. Proc. Natl. Acad. Sci. USA *76*, 514–517.

Bradke, F., and Dotti, C. G. (1998). Membrane traffic in polarized neurons. Biochim. Biophys. Acta *1404*, 245–258.

Brandan, E., Retamal, C., Cabello-Verrugio, C., and Marzolo, M. P. (2006). The low density lipoprotein receptor-related protein functions as an endocytic receptor for decorin. J. Biol. Chem. *281*, 31562–31571.

Bravo-Zehnder, M., Orio, P., Norambuena, A., Wallner, M., Meera, P., Toro, L., Latorre, R., and Gonzalez, A. (2000). Apical sorting of a voltage- and Ca^{2+}-activated K^+ channel alpha-subunit in Madin-Darby canine kidney cells is independent of N-glycosylation. Proc. Natl. Acad. Sci. USA *97*, 13114–13119.

Brown, M. D., Banker, G. A., Hussaini, I. M., Gonias, S. L., and Vandenberg, S. R. (1997). Low density lipoprotein receptor-related protein is expressed early and becomes restricted to a somatodendritic domain during neuronal differentiation in culture. Brain Res. *747*, 313–317.

Bu, G., and Marzolo, M. P. (2000). Role of rap in the biogenesis of lipoprotein receptors. Trends Cardiovasc. Med. *10*, 148–155.

Bu, G., Williams, S., Strickland, D. K., and Schwartz, A. L. (1992). Low density lipoprotein receptor-related protein/alpha 2-macroglobulin receptor is an hepatic receptor for tissue-type plasminogen activator. Proc. Natl. Acad. Sci. USA *89*, 7427–7431.

Burgos, P. V., Klattenhoff, C., de la Fuente, E., Rigotti, A., and Gonzalez, A. (2004). Cholesterol depletion induces PKA-mediated basolateral-to-apical transcytosis of the scavenger receptor class B type I in MDCK cells. Proc. Natl. Acad. Sci. USA *101*, 3845–3850.

Caceres, A., Banker, G., Steward, O., Binder, L., and Payne, M. (1984). MAP2 is localized to the dendrites of hippocampal neurons which develop in culture. Brain Res. *315*, 314–318.

Caceres, A., Mautino, J., and Kosik, K. S. (1992). Suppression of MAP2 in cultured cerebellar macroneurons inhibits minor neurite formation. Neuron *9*, 607–618.

Cameron, P. L., Südhof, T. C., Jahn, R., and Camilli, P. d. (1991). Colocalization of synaptophysin with transferrin receptors: implications of synaptic vesicle biogenesis. J. Cell Biol. *1991*, 151–164.

Cancino, J., Torrealba, C., Soza, A., Yuseff, M. I., Gravotta, D., Henklein, P., Rodriguez-Boulan, E., and Gonzalez, A. (2007). Antibody to AP1B adaptor blocks biosynthetic and recycling routes of basolateral proteins at recycling endosomes. Mol. Biol. Cell *18*, 4872–4884.

Casanova, J. E., Apodaca, G., and Mostov, K. E. (1991). An autonomous signal for basolateral sorting in the cytoplasmic domain of the polymeric immunoglobulin receptor. Cell *66*, 65–75.

Chen, W. J., Goldstein, J. L., and Brown, M. S. (1990). NPXY, a sequence often found in cytoplasmic tails, is required for coated pit-mediated internalization of the low density lipoprotein receptor. J. Biol. Chem. *265*, 3116–3123.

Cresawn, K. O., Potter, B. A., Oztan, A., Guerriero, C. J., Ihrke, G., Goldenring, J. R., Apodaca, G., and Weisz, O. A. (2007). Differential involvement of endocytic compartments in the biosynthetic traffic of apical proteins. EMBO J. *26*, 3737–3748.

Cuitino, L., Matute, R., Retamal, C., Bu, G., Inestrosa, N. C., and Marzolo, M.-P. (2005). ApoER2 is endocytosed by a clathrin-mediated process involving the adaptor protein Dab2 independent of its rafts association. Traffic *6*, 820–838.

Deborde, S., Perret, E., Gravotta, D., Deora, A., Salvarezza, S., Schreiner, R., and Rodriguez-Boulan, E. (2008). Clathrin is a key regulator of basolateral polarity. Nature *452*, 719–723.

Deora, A. A., Gravotta, D., Kreitzer, G., Hu, J., Bok, D., and Rodriguez-Boulan, E. (2004). The basolateral targeting signal of CD147 (EMMPRIN) consists of a single leucine and is not recognized by retinal pigment epithelium. Mol. Biol. Cell *15*, 4148–4165.

Dotti, C. G., Parton, R. G., and Simons, K. (1991). Polarized sorting of glypiated proteins in hippocampal neurons. Nature *349*, 158–161.

Dotti, C. G., and Simons, K. (1990). Polarized sorting of viral glycoproteins to the axon and dendrites of hippocampal neurons in culture. Cell *62*, 63–72.

Fiedler, K., and Simons, K. (1995). The role of N-glycans in the secretory pathway. Cell *81*, 309–312.

Folsch, H., Ohno, H., Bonifacino, J. S., and Mellman, I. (1999). A novel clathrin adaptor complex mediates basolateral targeting in polarized epithelial cells. Cell *99*, 189–198.

Folsch, H., Pypaert, M., Schu, P., and Mellman, I. (2001). Distribution and function of AP-1 clathrin adaptor complexes in polarized epithelial cells. J. cell Biol. *152*, 595–606.

Fullekrug, J., and Simons, K. (2004). Lipid rafts and apical membrane traffic. Ann. NY Acad. Sci. *1014*, 164–169.

Fuller, S. D., Bravo, R., and Simons, K. (1985). An enzymatic assay reveals that proteins destined for the apical and basolateral domains of an epithelial cell line share the same late Golgi compartments. EMBO J. *4*, 297–307.

Gan, Y., McGraw, T. E., and Rodriguez-Boulan, E. (2002). The epithelial-specific adaptor AP1B mediates post-endocytic recycling to the basolateral membrane. Nat. Cell Biol. *4*, 605–609.

Godyna, S., Liau, G., Popa, I., Stefansson, S., and Argraves, W. S. (1995). Identification of the low density lipoprotein receptor-related protein (LRP) as an endocytic receptor for thrombospondin-1. J. Cell Biol. *129*, 1403–1410.

Goretzki, L., and Mueller, B. M. (1998). Low-density-lipoprotein-receptor-related protein (LRP) interacts with a GTP-binding protein. Biochem. J. *336*, 381–386.

Gravotta, D., Deora, A., Perret, E., Oyanadel, C., Soza, A., Schreiner, R., Gonzalez, A., and Rodriguez-Boulan, E. (2007). AP1B sorts basolateral proteins in recycling and biosynthetic routes of MDCK cells. Proc. Natl. Acad. Sci. USA *104*, 1564–1569.

Griffiths, G., and Simons, K. (1986). The trans-Golgi network: sorting at the exit site of the Golgi complex. Science *234*, 4381–4443.

Herz, J., and Bock, H. H. (2002). Lipoprotein receptors in the nervous system. Annu. Rev. Biochem. *71*, 405–434.

Herz, J., Clouthier, D. E., and Hammer, R. E. (1992). LDL receptor-related protein internalizes and degrades uPA-PAI-1 complexes and is essential for embryo implantation [published erratum appears in Cell 1993 May 7;73(3): 428]. Cell *71*, 411–421.

Herz, J., Couthier, D. E., and Hammer, R. E. (1993). Correction: LDL receptor-related protein internalizes and degrades uPA-PAI-1 complexes and is essential for embryo implantation [letter]. Cell *73*, 428

Horton, A. C., and Ehlers, M. D. (2003). Neuronal polarity and trafficking. Neuron *40*, 277–295.

Hsu, D., Knudson, P. E., Zapf, A., Rolband, G. C., and Olefsky, J. M. (1994). NPXY motif in the insulin-like growth factor-I receptor is required for efficient ligand-mediated receptor internalization and biological signaling. Endocrinology *134*, 744–750.

Hunziker, W., and Fumey, C. (1994). A di-leucine motif mediates endocytosis and basolateral sorting of macrophage IgG Fc receptors in MDCK cells. EMBO J. *13*, 2963–2967.

Hussain, M. M. (2001). Structural, biochemical and signaling properties of the low-density lipoprotein receptor gene family. Front. Biosci. *6*, D417–D428.

Jareb, M., and Banker, G. (1998). The polarized sorting of membrane proteins expressed in cultured hippocampal neurons using viral vectors. Neuron *20*, 855–867.

Kreitzer, G., Marmorstein, A., Okamoto, P., Vallee, R., and Rodriguez-Boulan, E. (2000). Kinesin and dynamin are required for post-Golgi transport of a plasma-membrane protein. Nat. Cell Biol. *2*, 125–127.

Le Bivic, A., Real, F. X., and Rodriguez-Boulan, E. (1989). Vectorial targeting of apical and basolateral plasma membrane proteins in a human adenocarcinoma epithelial cell line. Proc. Natl. Acad. Sci. USA *86*, 9313–9317.

Le Gall, A. H., Powell, S. K., Yeaman, C. A., and Rodriguez-Boulan, E. (1997). The neural cell adhesion molecule expresses a tyrosine-independent basolateral sorting signal. J. Biol. Chem. *272*, 4559–4567.

Li, Y., Lu, W., Marzolo, M. P., and Bu, G. (2001a). Differential functions of members of the low density lipoprotein receptor family suggested by their distinct endocytosis rates. J. Biol. Chem. *276*, 18000–18006.

Li, Y., Marzolo, M. P., Kerkhof, P., Strous, G. J., and Bu, G. (2000). The YXXL motif, but not the two NPXY motifs, serves as the dominant endocytosis signal For LDL receptor-related protein (LRP). J. Biol. Chem. *275*, 17187–17194.

Li, Y., van Kerkhof, P., Marzolo, M. P., Strous, G. J., and Bu, G. (2001b). Identification of a major cyclic AMP-dependent protein kinase A phosphorylation site within the cytoplasmic tail of the low-density lipoprotein receptor-related protein: implication for receptor-mediated endocytosis. Mol. Cell. Biol. *21*, 1185–1195.

Lock, J. G., and Stow, J. L. (2005). Rab11 in recycling endosomes regulates the sorting and basolateral transport of E-cadherin. Mol. Biol. Cell *16*, 1744–1755.

Marmorstein, A. D., Csaky, K. G., Baffi, J., Lam, L., Rahaal, F., and Rodriguez-Boulan, E. (2000). Saturation of, and competition for entry into, the apical secretory pathway. Proc. Natl. Acad. Sci. USA *97*, 3248–3253.

Marzolo, M. P., Bull, P., and Gonzalez, A. (1997). Apical sorting of hepatitis B surface antigen (HBsAg) is independent of N-glycosylation and glycosylphosphatidylinositol-anchored protein segregation. Proc. Natl. Acad. Sci. USA *94*, 1834–1839.

Marzolo, M. P., Yuseff, M. I., Retamal, C., Donoso, M., Ezquer, F., Farfan, P., Li, Y., and Bu, G. (2003). Differential distribution of low-density lipoprotein-receptor-related protein (LRP) and megalin in polarized epithelial cells is determined by their cytoplasmic domains. Traffic *4*, 273–288.

Matter, K., Hunziker, W., and Mellman, I. (1992). Basolateral sorting of LDL receptor in MDCK cells: the cytoplasmic domain contains two tyrosine-dependent targeting determinants. Cell *71*, 741–753.

Matter, K., and Mellman, I. (1994). Mechanisms of cell polarity: sorting and transport in epithelial cells. Curr. Opin. Cell Biol. *6*, 545–554.

Matter, K., Whitney, J. A., Yamamoto, E. M., and Mellman, I. (1993). Common signals control low density lipoprotein receptor sorting in endosomes and the Golgi complex of MDCK cells. Cell *74*, 1053–1064.

Matter, K., Yamamoto, E. M., and Mellman, I. (1994). Structural requirements and sequence motifs for polarized sorting and endocytosis of LDL and Fc receptors in MDCK cells. J. Cell Biol. *126*, 991–1004.

Mostov, K. E. (2003). Epithelial polarity and morphogenesis. Methods *30*, 189–190.

Mostov, K. E., and Cardone, M. H. (1995). Regulation of protein traffic in polarized epithelial cells. Bioessays *17*, 129–138.

Müsch, A., Xu, H., Schields, D., and Rodriguez-Boulan, E. (1996). Transport of vesicular stomatitis virus G protein to the cells surface is signal mediated in polarized and nonpolarized cells. J. Cell Biol. *133*, 543–558.

Obermoeller, L. M., Chen, Z., Schwartz, A. L., and Bu, G. (1998). Ca^{2+} and receptor-associated protein are independently required for proper folding and disulfide bond formation of the low density lipoprotein receptor-related protein. J. Biol. Chem. *273*, 22374–22381.

Odorizzi, G., and Trowbridge, I. S. (1997). Structural requirements for basolateral sorting of the human transferrin receptor in the biosynthetic and endocytic pathways of Madin-Darby canine kidney cells. J. Cell Biol. *137*, 1255–1264.

Ohno, H., Tomemori, T., Nakatsu, F., Okazaki, Y., Aguilar, R. C., Foelsch, H., Mellman, I., Saito, T., Shirasawa, T., and Bonifacino, J. S. (1999). Mu1B, a novel adaptor medium chain expressed in polarized epithelial cells. FEBS Lett. *449*, 215–220.

Paglini, G., Pigino, G., Kunda, P., Morfini, G., Maccioni, R., Quiroga, S., Ferreira, A., and Caceres, A. (1998). Evidence for the participation of the neuron-specific CDK5 activator P35 during laminin-enhanced axonal growth. J. Neurosci. *18*, 9858–9869.

Pietrini, G., Suh, Y. J., Edelmann, L., Rudnick, G., and Caplan, M. J. (1994). The axonal gamma-aminobutyric acid transporter GAT-1 is sorted to the apical membranes of polarized epithelial cells. J. Biol. Chem. *269*, 4668–4674.

Rindler, M. J., Ivanov, I. E., Plesken, H., Rodriguez-Boulan, E., and Sabatini, D. D. (1984). Viral glycoproteins destined for apical or basolateral plasma membrane domains traverse the same Golgi apparatus during their intracellular transport in doubly infected Madin-Darby canine kidney cells. J. Cell Biol. *98*, 1304–1319.

Rodriguez-Boulan, E., and Gonzalez, A. (1999). Glycans in post-Golgi apical targeting: sorting signals or structural props? Trends Cell Biol. *9*, 291–294.

Rodriguez-Boulan, E., Kreitze, G., and Musch, A. (2005). Organization of vesicular trafficking in epithelia. Nat. Rev. Mol. Cell Biol. *6*, 233–247.

Rodriguez-Boulan, E., and Powell, S. K. (1992). Polarity of epithelial and neuronal cells. Annu. Rev. Cell Biol. *8*, 395–427.

Roebroek, A. J., Reekmans, S., Lauwers, A., Feyaerts, N., Smeijers, L., and Hartmann, D. (2006). Mutant Lrp1 knock-in mice generated by recombinase-mediated cassette exchange reveal differential importance of the NPXY motifs in the intracellular domain of LRP1 for normal fetal development. Mol. Cell. Biol. *26*, 605–616.

Rosso, S., Bollati, F., Bisbal, M., Peretti, D., Sumi, T., Nakamura, T., Quiroga, S., Ferreira, A., and Caceres, A. (2004). LIMK1 regulates Golgi dynamics, traffic of Golgi-derived vesicles, and process extension in primary cultured neurons. Mol. Biol. Cell *15*, 3433–3449.

Salicioni, A. M., Mizelle, K. S., Loukinova, E., Mikhailenko, I., Strickland, D. K., and Gonias, S. L. (2002). The low density lipoprotein receptor-related protein mediates fibronectin catabolism and inhibits fibronectin accumulation on cell surfaces. J. Biol. Chem. *277*, 16160–16166.

Silverman, M. A., Peck, R., Glover, G., He, C., Carlin, C., and Banker, G. (2005). Motifs that mediate dendritic targeting in hippocampal neurons: a comparison with basolateral targeting signals. Mol. Cell Neurosci. *29*, 173–180.

Simmen, T., Honing, S., Icking, A., Tikkanen, R., and Hunziker, W. (2002). AP-4 binds basolateral signals and participates in basolateral sorting in epithelial MDCK cells. Nat. Cell Biol. *4*, 154–159.

Soza, A., Norambuena, A., Cancino, J., De La Fuente, E., Henklein, P., and Gonzalez, A. (2004). Sorting competition with membrane-permeable peptides in intact epithelial cells revealed discrimination of transmembrane proteins not only at the trans-golgi network but also at pre-golgi stages. J. Biol. Chem. *279*, 17376–17383.

Stockinger, W., Sailler, B., Strasser, V., Recheis, B., Fasching, D., Kahr, L., Schneider, W. J., and Nimpf, J. (2002). The PX-domain protein SNX17 interacts with members of the LDL receptor family and modulates endocytosis of the LDL receptor. EMBO J. *21*, 4259–4267.

Sugimoto, H. *et al.* (2002). Differential recognition of tyrosine-based basolateral signals by AP-1B subunit mu1B in polarized epithelial cells. Mol. Biol. Cell *13*, 2374–2382.

van Kerkhof, P., Lee, J., McCormick, L., Tetrault, E., Lu, W., Schoenfish, M., Oorschot, V., Strous, G. J., Klumperman, J., and Bu, G. (2005). Sorting nexin 17 facilitates LRP recycling in the early endosome. EMBO J. *24*, 2851–2861.

Wilson, J. M., de Hoop, M., Zorzi, N., Toh, B. H., Dotti, C. G., and Parton, R. G. (2000). EEA1, a tethering protein of the early sorting endosome, shows a polarized distribution in hippocampal neurons, epithelial cells, and fibroblasts [In Process Citation]. Mol. Biol. Cell *11*, 2657–2671.

Winckler, B., and Mellman, I. (1999). Neuronal polarity: controlling the sorting and diffusion of membrane components. Neuron *23*, 637–640.

Worby, C. A., and Dixon, J. E. (2002). Sorting out the cellular functions of sorting nexins. Nat. Rev. Mol. Cell Biol. *3*, 919–931.

Yap, C. C., Murate, M., Kishigami, S., Muto, Y., Kishida, H., Hashikawa, T., and Yano, R. (2003). Adaptor protein complex-4 (AP-4) is expressed in the central nervous system neurons and interacts with glutamate receptor delta2. Mol. Cell Neurosci. *24*, 283–295.

Yeaman, C., Grindstaff, K. K., and Nelson, W. J. (1999). New perspectives on mechanisms involved in generating epithelial cell polarity. Physiol. Rev. *79*, 73–98.

Zhuo, M., Holtzman, D. M., Li, Y., Osaka, H., DeMaro, J., Jacquin, M., and Bu, G. (2000). Role of tissue plasminogen activator receptor LRP in hippocampal long-term potentiation. J. Neurosci. *20*, 542–549.